DEVELOPMENT OF WEAR RESISTANT EXTRUSION DIES

Daniel O'Brien

Bachelor of Engineering
Mechanical Engineering

MACQUARIE
University

Department of Engineering
Macquarie University

November 5th, 2017

Supervisor: Prof Candace Lang

ACKNOWLEDGEMENTS

I would like to acknowledge a number of people who helped me not only during this thesis but my entire undergraduate degree.

Firstly, I would like to thank my family and partner Rachael. Your support and understanding throughout my studies has been amazing and your constant encouragement towards my learning has enabled me to achieve my full potential.

Next, I would like to say a huge thank you to my supervisor professor Candace Lang. Your guidance throughout this entire thesis has been invaluable and your flexibility in regards to the project direction and consultation times were truly appreciated. Alongside Candace I would like to thank a number of staff members at Macquarie University, in particular Wendy Tao who made the use of labs and equipment easily accessible, and Sue Lindsay and the team at the m-unit who helped make sense of numerous test samples.

Finally, a big thankyou to Capral / Austex Dies, in particular Alessandro Ferrari. The project would not have been possible without the dies and advice you supplied. Your help in generating background knowledge on the subject and your willingness to answer any question I threw at you is greatly appreciated.

STATEMENT OF CANDIDATE

I, Daniel O'Brien, declare that this report, submitted as part of the requirement for the award of Bachelor of Engineering in the Department of Mechanical Engineering, Macquarie University, is entirely my own work unless otherwise referenced or acknowledged. This document has not been submitted for qualification or assessment at any academic institution.

Student's Name: Daniel O'Brien

Student's Signature:

Date: 5th August 2017

ABSTRACT

Dies used for the production of aluminium extrusions are subjected to varying degrees of mechanical and chemical degradation. Dies themselves are costly and time consuming to produce, hence from the perspective of the user it is desirable for them to have a significant lifespan. A review of literature suggests that a significant factor in improving the mechanical properties of a die are through the use of various heat treatments, in conjunction with several surface hardening techniques. Here we examine the effectiveness of this through various case studies as well as experimental results, all of which will be performed on dies that have been subjected to the extrusion process previously.

The importance of some form of surface coating that can be re-applied over the life of the die will be looked at. It is through the examination of this that we will highlight how future advances in creating longer lasting dies, will come from the development of technologies that allow for constant and accurate measurement of this protective surface treatment.

CONTENTS

ACKNOWLEDGEMENTS ..... **III**

ABSTRACT ..... **VII**

CONTENTS ..... **IX**

LIST OF FIGURES ..... **X**

LIST OF TABLES ..... **XII**

1. INTRODUCTION **1**
1.1. Project Goal **2**

2. LITERATURE REVIEW **3**
2.1 AISI H13 Tool steel. **3**
2.2 Degradation Of Extrusion Dies **5**
2.3 Heat Treatment **6**
2.4 Application Of Surface Treatments **9**
2.4.1 Nitriding 9
2.4.2 Physical Vapor Deposition Coatings And Duplex Coatings 11
2.4.3 Implications Of Surface Treatments For Prolonged Die Life 13
2.4.4 Measuring The Extent And Life Expectancy Of The Surface Hardening Treatment 14

3. EXPERIMENTAL METHODS **16**
3.1 Sample Preparation **16**
3.2 Hardness Testing **19**
3.3 Etching The Samples **23**
3.4 Scanning Electron Microscopy (SEM) And Energy-Dispersive X-Ray Spectroscopy (EDS). **24**

4. RESULTS **25**

5. DISCUSSION **44**

6. CONCLUSION **57**

7. FUTURE WORK **61**

8. REFERENCES **62**

9. APPENDIX **64**
[1] H13 Tool Steel Datasheet (Provided by Austex Dies) 64
[2] Attendance Form 65

LIST OF FIGURES

Figure 1 Iron carbon phase diagram for carbon steel[1] 8
Figure 2 Determination of nitride hardness depth (NHD)[3] 15
Figure 3 Engineering drawing of die provided by Austex dies sowing section cuts and cross section through it. 16
Figure 4 Reference image for sectioning die showing cut location and sample locations. 17
Figure 5 Calculation of area of hardness indent 19
Figure 6 Hardness indenter parameters 19
Figure 7 Microhardness test results for sample 1 lot1 bearing surface analysis .20
Figure 8 Microhardness test results sample 3 lot1 cross section through bearing surface 20
Figure 9 Sample 1 Etched in 2% Nital Solution 23
Figure 10 Sample 4 Etched in 4% Nital Solution 23
Figure 11 "Sample 1 (Lot1)" Microstructure of bearing surface of the die etched in 2% Nital solution. 25
Figure 12 "Sample 4(Lot1)" Microstructure of surface of Die etched in 4% Nital solution. 26
Figure 13 "Sample 2 (Lot1)" Microstructure behind leading edge of bearing surface at a corner. 27
Figure 14 Reference image for figure 14 28
Figure 15 "Sample 2(Lot1)" Bearing surface at corner of die. 28
Figure 16 EDS Mapping of “Sample 2 (Lot1)” 29
Figure 17 EDS Spectrum data “Sample 2 (Lot1)” 30
Figure 18 Nitrogen dispersion through sample 2 31
Figure 19 Sample 4 Microstructure composition analysis "Spot 1" 33
Figure 20 Sample 4 Microstructure composition analysis "Spot 2" 33
Figure 21 Microstructure composition analysis comparison between various regions on dies surface. 34
Figure 22 Composition analysis comparison for points shown in figure 21. 34
Figure 23 Sample cut from surface of die (Section 15 see figure 4) 35

Figure 24 SEM image sample shown in figure 20 (30 Micron Scale).....36
Figure 25 Combined EDS mapping of sample show in figure 20.....36
Figure 26 EDS Composition analysis of element distribution from sample show in figure 20.....37
Figure 27 Pearlite microstructure evident in "sample1(Lot2)" taken from bearing surface of die.....38
Figure 28 Hardness results sample 1 lot 2 bearing surface analysis.....40
Figure 29 Hardness test results for comparison of nitrided surface and underlying material.....40
Figure 30 Sample 1 location 2 bearing surface (Lot2.....42
Figure 31 Sample 1location 1 bearing surface (Lot2).....42
Figure 32 Sample 1 location 3 bearing surface (Lot2).....43
Figure 33 Sample 1 location 4 bearing surface (Lot2).....43
Figure 34 Corrosion and removal of material from bearing surface of the die (100 μm Scale).....48
Figure 35 Corrosion and removal of material from surface of the die (100 μm Scale).....48
Figure 36 Measuring nitride layer depth through hardness test[2].....50
Figure 37 Graphical representation of data in table 14. Shows the trend of consistent hardness readings with increasing indenter force, for non nitrided samples.....54
Figure 38 Graphical representation of data in table 13. Shows trend of increasing hardness indent depth with increasing test force, leading to a decreasing overall hardness for nitrided sample.....54
Figure 39 Visualisation and graphical measurement of nitride layer thickness...56

LIST OF TABLES

Table 1 Composition of H13 tool steel (Die Provided by Austex, composition obtained through the use of EDS) 3
Table 3 Heat treatment process tested dies have undergone in accordance with data provided by Austex dies. [14] 6
Table 4 Sample names and locations in which they were cut from (" Lot 1") 17
Table 5 Sample sames and locations in which they were cut from (" Lot 2") 17
Table 6 Grinding and Polishing Procedure for Samples [4]. 18
Table 7 EDS composition analysis “Sample 2 (Lot1)” 30
Table 8 EDS "Spot 1" Composition red highlighted region 33
Table 9 EDS "Spot 2" Composition red highlighted region 33
Table 10 EDS "Spot 3" Composition analysis orange highlighted region 34
Table 11 EDS composition of sample shown in figure 20 36
Table 12 EDS Composition analysis for sample show in figure 24 (Average element concentration over map) 36
Table 13 Hardness indent depth calculations for surface of die for sample shown in figure 23 52
Table 14 Hardness indent depth calculations for Sample 1 lot 1 53

1. INTRODUCTION

Today as a society we produce more aluminium than all other nonferrous metals combined [1][5]. By weight it makes up 8% of the earth's crust meaning that it is the third most abundant element behind silicon and air. The applications of aluminium from an engineering perspective are almost endless and this is largely due to its diverse range of properties. Aluminium amongst other things has a high strength to weight ratio, is impermeable to matter such as air and microorganisms, is corrosion resistant, non-magnetic and possesses high amounts of flexibility [2][6]. It is a combination of these properties that has allowed aluminium to find a place as a perfect material to use for extrusions in a variety of industries.

The extrusion process calls for a pre-heated aluminium billet to be forced through an opening in the surface of a die at high heat and pressure. This process allows for the creation of many geometries not achievable through conventional manufacturing techniques. It offers the ability to generate seamless profiles with an excellent surface finish.

The process of extrusion exposes the dies to severe thermal, mechanical and chemical stresses from both the friction generated between the sliding surfaces, and the magnitude of the force required to extrude the material [3] [7]. These conditions dictate that the die must be of suitable hardness in order to achieve its purpose. The hardness characteristics of an extrusion die are almost exclusively imparted through the use of various heat treatments and surface hardening techniques. An aluminium extrusion die is typically constructed from AISI (American Iron and Steel Institute) H13 Tool Steel [8]. The general heat treatment procedure for the hardening of tool steel usually involves preheating followed by an extended soaking period before quenching and multiple tempering treatments. Finally it undergoes some form of nitriding or similar surface hardening treatment.

The nitriding process applied to the die is usually achieved through one of several techniques including gas, plasma or salt-bath nitriding, all of which are explored in depth throughout the paper. Nitriding is the preferred surface hardening method used for extrusion dies. It is a critical step in reducing premature degradation of the die, it involves the application of a hardened superficial layer that minimises friction and wear to the bearing surface of a die.

1.1. Project Goal.

The goal of this project is ultimately to develop an aluminium extrusion die with an extended life.

To achieve this an examination of current heat treatment methods performed on dies (provided by Austex Dies) will be conducted, assessing the corresponding mechanical properties imparted by the respective heat treatment. Alongside this I will assess surface hardening techniques that could possibly be re-applied over the life of the die to further prolong its life. In conducting this analysis, I hope to observe possible flaws or points of improvement.

A literature review on the topic reveals the magnitude of this industry and suggests that this is a continuing process as manufacturers constantly try to get more out of each die. As a result of this it was decided to target specific regions for improvement rather than experiment with completely new treatment processes.

2. LITERATURE REVIEW

2.1 AISI H13 Tool steel.

H13 tool steel belongs to the H group of steels (hot working group). It is given this designation due to chromium and molybdenum being the major alloying elements. H13 is the most widely used material for the manufacturing of extrusion dies [3]. The preference to use H13 is largely due to its high levels of hardness, fixed with excellent resistance to thermal fatigue and crack propagation. The material itself is a steel alloy consisting of higher concentrations of chromium, silicon, molybdenum and vanadium [5].

Austex dies provided a sample aluminium extrusion die for testing and experimentation. A scanning electron microscope utilising composition analysis was used to give an accurate representation of the samples' composition, with the results detailed in table 1 below. (See Appendix 1 for Material Data sheet).

Table 1 Composition of H13 tool steel (Die Provided by Austex, composition obtained through the use of EDS)

Element Number	Element Symbol	Element Name	Atomic Conc.	Weight Conc.
6	C	Carbon	20.32	6.87
24	Cr	Chromium	3.24	4.74
14	Si	Silicon	1.28	1.01
42	Mo	Molybdenum	0.70	1.88
23	V	Vanadium	0.53	0.76

Table 2 Standard American Iron & Steel Institute (AISI) H13 Tool Steel Composition[9]

Element	Iron	Carbon	Chromium	Silicon	Manganese	Vanadium	Molybdenum
%	Balance	0.32-0.45	4.75-5.5	0.8-1.2	0.2-0.5	0.8-1.2	1.1-1.75

Comparison of results from both tables 1 and 2 shows that the composition of the supplied test die is within the accepted range for AISI H13 tool steel, with the exception of carbon. The increase in carbon concentration of the test sample could however be attributed to the fact that the sample die has already undergone a series of heat treatments as well as a nitriding surface hardening

process. This would explain a slight rise in carbon concentration within the sample and it is something that will be investigated further.
In addition it should be noted however that the carbon composition obtained via the EDS feature within a scanning electron microscope in table 1 has been well documented to be difficult to measure. This could also explain the more significant variances in the detection of carbon.

In terms of its composition, each of the alloying elements brings desired mechanical properties to the steel. The material's increased hardness is largely attributed to molybdenum. Increased silicon content increases resistance to oxidation during heating of the steel, whilst the addition of vanadium actually decreases the material's hardness, however it gives rise to an increase in toughness, as it draws in carbon to form vanadium carbides throughout the steel [10].

2.2 Degradation Of Extrusion Dies

The wear of an extrusion die is brought about by the interaction of various surfaces in motion. It is the progressive removal of a die's bearing surface layer; this in turn means that the die's geometry is altered causing variances in material flow over the face of the die [11]. The nature of extrusion means that the aluminium has a tendency to adhere to the steel die. Not only does this cause an increase in friction, it is responsible for the chemical degradation of its surface as the two dissimilar metals come into contact and subsequently lead to wear. This is where we begin to see the importance of some form of surface hardening technique. Not only does it harden the material, making it more resistant to thermal stress, it alters the tribological interactions between the surfaces, reducing friction and chemical degradation [4]. In order to minimise the wear a die suffers during extrusion we must consider a careful balance of several factors.

The adhesive wear brought on by aluminium's tendency to stick to the steel die is a direct result of the extrusion rate and pressure of extrusion. The premature wear of a die has not only technical implications in terms of tolerances and cross-sectional variances, but economically it becomes less viable to run the die as an increased mass of material is required for the same length extrusion.

2.3 Heat Treatment

Heat treatment from a metallurgy perspective is defined as a series of processes involving heating at predetermined rates, soaking at elevated temperatures for a set duration of time, followed by a period of cooling within a specific medium at another predetermined rate [6] [12].

The following table depicts the heat treatment process the tested dies were subjected to. It should be noted that Fluidised Bed Furnaces (FBF) are used for the treatment of the dies. The process involved the use of multiple furnaces in the preheating and hardening phases of treatment. Because of this I ensured that temperature variances within the furnaces were assessed and found to have negligible effect on the treatment of the dies.

A fluidised bed furnace works by fluidising particles within the furnace. This is achieved through the injection of a combustible gas along with oxygen through holes within the base and wall of the furnace [13]. Such a furnace is highly efficient in the transfer of both thermal and chemical energy.

Table 3 Heat treatment process tested dies have undergone in accordance with data provided by Austex dies. [14]

Process	Description
Initial Preheat	For the initial preheating the dies are heated somewhere between 550-600°C for 1.5 Hours (Furnace 1).
Secondary Preheat	The dies are then moved to a secondary furnace where they are further preheated to 860°C for another 2 hours (Furnace 2).
Hardening	Hardening of the dies is achieved by soaking at 1020°C for 1.5 hours in furnace 2 (It takes 1 hour to reach temperature then there is 20-30 min soaking time).
Quench	Quench is achieved when final temperature is measured as 50°C (This equates to approximately 1.5-2 hours for a 200-250Kg load).
Initial Tempering	Dies are heated to 530°C for 4.5 hours
1st Air/Quenching	Once the initial tempering is completed they are quenched in air and left to cool to room temperature.
Secondary Tempering	The dies are again heated, this time to 590°C and left to soak for 4 hours (this gives an expected hardness of 46-48 HRC).
2nd Air/Quenching	At the end of the second temper the dies are again quenched in air and allowed to cool to room temperature.

Final hardness testing on the dies is done after the 2nd air quench but only once the dies have reached room temperature. This is done to ensure that the required hardness 46-48 HRC has been met. Further analysis is conducted later in the report to verify these hardness readings. Several measurements are taken from various sections of the die, giving an overall view to the degree of hardening imparted as a result of the specified heat treatment in table 3 above.

Referring to table 3, the initial heating of the dies to 1020°C is done above the eutectoid temperature. Soaking at this elevated temperature (austenitizing temperature) causes a phase change. The Body Center Cubic (BCC) ferrite structure transitions to a gamma phase iron, more commonly known as austenite (See figure 1). This allotrope of iron is stable whilst above the eutectoid temperature. As the die is allowed to cool we again see a phase transition within the metal.

As the Austenite is cooled we begin to see a diffusion of Carbon into the alloy, allowing the formation of iron carbide or Cementite. The rate at which the die is allowed to cool dramatically affects its microstructure and consequently its mechanical properties. A quicker quenching of the die results in less carbon diffusing within the alloy, leading to the formation of martensite. The martensitic structure is a significantly harder region within the steel, however its presence distorts the crystalline lattice due to the fact that the cooling is usually uneven throughout the cross section of the material. This is because the extremities cool faster than the internals of the die. As well as this we see variances in volumes as martensite is less dense than the surrounding austenite. These factors compound leading to an increase in the internal stress within the die. This is obviously not ideal and hence we must carefully monitor the cooling rate allowing the temperature to decrease at a uniform rate throughout the die [7][15].

As a result of the hardening process we have a steel that whilst being considerably harder, is significantly more brittle. Again, for an extrusion die this is not ideal. Whilst the aim is to have high hardness, the nature of the extrusion process dictates that a brittle material will fail under the force of extrusion.

To combat this a tempering process takes place. This involves again heating the die, this time below the eutectoid temperature and allowing it to cool at a slower set rate.

Here we sacrifice excess hardness for an increase in toughness. The amount of hardness removed is dictated by temperature at which the metal is tempered at.

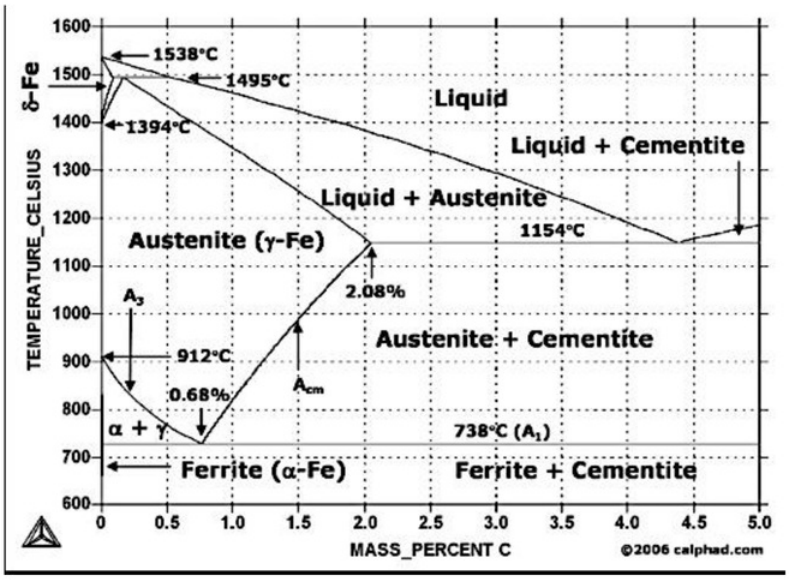

Figure 1 Iron carbon phase diagram for carbon steel[1]

2.4 Application Of Surface Treatments

2.4.1 Nitriding

One mechanism employed within the industry to prolong the life of an extrusion die is through the application of a thermochemical treatment [16]. Nitriding as a means of surface hardening an extrusion die is one of the most common practices employed to prolong its life. Several mechanisms are used to achieve a nitrided surface layer some of which include; salt-bath nitriding, gas nitriding and plasma or ionic nitriding [17].

Gas nitriding is achieved by transferring nitrogen from an atmosphere enriched with ammonia to a steel, heated between the ferrite and carbide regions (see figure 1) [18]. Ionic nitriding is a multistep process. Firstly the specimen is placed in a vacuum before being back filled with a process gas. This allows for the preheating of the material. From here a voltage is applied to the process gas, ionising it. The ionisation process is aimed at stripping and cleaning the materials' surface of any impurities. Following on, controlled amounts of nitrogen methane and hydrogen are pumped into the chamber hence beginning the nitriding process [19].

The result of either process is the formation of what is known as the white layer. This is an ε/γ' iron-nitride compound layer. In its simplest form the compound layer can be visualized as a series of stages:

1. Firstly we see Nitrogen being absorbed by the alpha ferrite (α-Fe)
2. Once solubility is reached within the ferrite region we see the formation of gamma prime (γ'-Fe).
3. Finally, solubility within the γ' region is reached and we see the formation of epsilon-iron [20-22].

Beneath the white layer lies the diffusion zone. Here we can observe epsilon-iron (ε-$Fe_{2\text{-}3}$). The epsilon-iron is formed as nitrogen from the surface is absorbed within the ferrite lattice, in turn reacting with the carbides within the alloy. The diffusion zone has increased hardness over the substrate material as it is a combination of some solid solution of the base material and some regions of precipitation hardening [18].

Some literature would suggest that it is arguable as to the exact effectiveness of the white layer, as it may be seen to have undesirable characteristics as highlighted in [23]. Whilst we see a significant increase in the hardness, the surface of the material is subsequently made more brittle. During extrusion this hardened superficial surface may fracture, causing imperfections in the extrusion profile and premature oxidation of the die. As a result of this, the process must be carefully controlled in order to diffuse the correct amounts of nitrogen into the material so as to achieve the desired mechanical properties. Conversely it has also been argued in the case of alloyed steels such as H13, that with higher concentrations of nitride forming elements such as chromium, vanadium and molybdenum, it should be noted that nitriding greatly improves the mechanical properties of such a material [18]. This article also raises the point that from a thermodynamic and kinetic perspective we have little understanding on the exact extent of the nitriding process on alloyed steels, which aligns with the work presented in Björk's research in [23].

2.4.2 Physical Vapor Deposition Coatings And Duplex Coatings

An alternative method of surface hardening that has seen an increased use in surface hardening for extrusion dies is Physical Vapor Deposition coatings (PVD). PVD utilises no chemicals in order to harden the material. Hardening is achieved through vaporisation of a target material and condensing it on a substrate [24]. All PVD coatings are applied within a vacuum and have the advantage of being able to be precisely controlled. Surface thickness can be varied from several atomic layers to 15μm, and in addition there are a wide variety of coatings that can be used in to target specific material needs.

The Need for PVD coating has become apparent as we require a greater life span from each die. A typical extrusion die has the capacity to produce approximately (20-50) $\times 10^3$ M worth of extrusions [25]. In many cases simply nitriding the dies is not sufficient. The application of duplex coatings such as PVD and nitriding is aimed at reducing the friction and subsequent abrasion between the surfaces. The application of PVD coatings such as Chromium Nitride(CrN), Titanium Nitride(TiN) and Titanium DiBoride (TiB_2) are all explored in literature such as [25]. Experiments were conducted with samples of H13 tool steel. Some samples were nitrided whilst others were given duplex PVD coatings (Nitriding and PVD). Finally some samples were prepared with no surface hardening. An apparatus (ball on disk test) was used to simulate the extrusion process and observe the wear on each sample. The results suggested samples with PVD coatings performed, on average, 10 times better than a conventional salt bath nitrided sample. It also concluded that the successful PVD coatings all displayed chemical resistance to the adhesion and friction from the aluminum, which was observed to be more important than a greater hardness overall. The conclusions drawn on in [25] are further justified in [26]. A similar experiment was conducted and again concluded that the wear resistance of a PVD coated extrusion die is several orders of magnitude greater than that of an uncoated one.

Whilst [23 -24] draw conclusions that the application of a PVD coating is entirely beneficial, points such as those drawn upon in [27] must be considered. The application of a PVD coating on its own without prior surface treatment can in fact lead to degradation of the die at an accelerated rate. As noted, the main differentiating factor between a PVD treatment and a nitriding process is that PVD utilises no chemical reactions to harden the material. As a result we see a large hardness gradient between the applied coating and the substrate material. This usually dictates that the adhesion between the two materials will be poor, resulting in a failure of the treatment during extrusion. [27] Looks at exactly this. It compares un-treated samples to those that have a duplex surface hardening treatment, as well as comparing various heat treatment methods for each.

The results found that variances in the heat treatment methods produced only slight variances in the sample's microstructure. Both heat treatments tested produced samples with a perlite microstructure. It was also found that at low temperature and low load capacity no great variances were observed in the wear behavior of the tested samples, however at elevated temperatures and loads the duplex treated samples were the only ones to display no wear after testing. Also to be noted, it was found that when comparing a nitrided sample to one containing a single layer PVD coating, the nitrided sampled displayed five times better wear resistance, further emphasising the point that a PVD only coated sample may suffer from degradation at a quicker rate.

2.4.3 Implications Of Surface Treatments For Prolonged Die Life

It is quite evident that surface treatments play a crucial rule in extending the life of an extrusion die. There is significant literature that details the advantages of surface hardening, however it is suggested that when dealing with high alloy steels, the extent and exact effectiveness of nitriding is not entirely clear [23]. This is something that should be further explored. The observed results from various case studies all suggest that nitriding does in fact increase the load carrying capacity of the material in terms of its resistance to wear at elevated temperatures and forces. It acts as a bridge to decrease the hardness gradient between the substrate and coating material if a duplex treatment is used alongside this. Its chemical composition means that the oxide layer formed during the process acts to hinder any further oxidation that occurs in almost all metal interactions at elevated temperatures.

The application of multiple surface hardening techniques and their ability to extend the life of a die, 10 fold in some cases [25], has clearly already been noted. However, experimental reports rarely express the cost of such procedures. Industry users of such dies place significant consideration on the cost versus gain analysis of a product. So whilst we may be able to increase the wear resistance of the die, unless the profit it will generate outweighs the cost of the coating procedure by a sufficient factor, such a coating would be useless.

2.4.4 Measuring The Extent And Life Expectancy Of The Surface Hardening Treatment.

A key step to moving forward in developing longer lasting dies is monitoring the state of the die, more specifically the thickness of its surface treatment. We have already established that due to the nature of the process it is imperative that the dies have some form or surface hardening treatment. This acts as the first and primary means to limit the effects of the tribological integrations between the tool and the aluminum extrusion, hence it makes sense to gain the most out of this protective coating in order to maximise the life of the die. Later in the report I look at the extent of the damage the bearing surface has sustained as a result of the extrusion process, and it will become evident the need to develop methods to quickly ascertain the condition of the protective surface treatments.

The application of multiple nitriding processes over the life of an extrusion die is already a common practice used to increase its service life. At present the most common practice to ascertain an understanding into the effectiveness of a hardening process on a material is to perform a series of hardness tests. When assessing a material that has a surface hardening treatment we look for two key elements; effective surface depth and total case depth. [28]

- Effective case depth being a point within the material up to which an elevated level of hardness is maintained.
- Total case depth being the point within the material after which there is no change in the materials' hardness and it is considered uniform.

It is through analysis of these parameters that we are able to determine the nitride hardness depth. Standard DIN 50190-3 defines the process used to calculate the nitride hardness depth as shown in the following figure. [29]

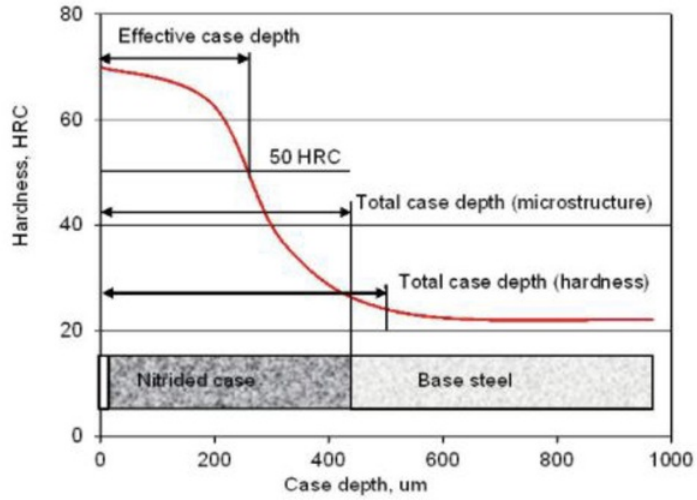

Figure 2 Determination of nitride hardness depth (NHD)[3]

Whilst this gives us a fair indication as to the overall hardness profile of the extrusion die, it is far from specific. We have already established that the nitriding process can have an inconsistent nature in terms of even distribution, particularly as the die's geometry becomes more intricate. We have also noted that deposition techniques are a line of sight process, which again is hindered by complex geometry.

One of the major factors that needs consideration in order to improve the surface hardening mechanisms for extrusion dies will be in the development of non-destructive ways in which to measure the depth and consistency of surface treatments. Developments of such technologies will enable the dies' users to quickly ascertain the condition of the die and assess if the application of a surface treatment is necessary in order to repair the die before it gets to the point where it is no longer rendered cost effective.

3. EXPERIMENTAL METHODS

3.1 Sample Preparation

The sample die was initially sectioned into smaller areas as shown in figure 3 below. The die was difficult to cut due to its complex geometry and increased hardness. The initial sectioning cuts were made using a horizontal ban saw and large amounts of cutting fluid. Care was taken when sectioning the die so as to cut it in such a way that the blade did not affect the bearing surface I wished to examine (see figure 3 section AA). The die was cut at a slow and constant speed avoiding excess heat build-up and failure of the cutting blade. When sectioning the die, care was taken to ensure that the bearing surface in which I wished to examine was left intact and free from any possible tool marks.

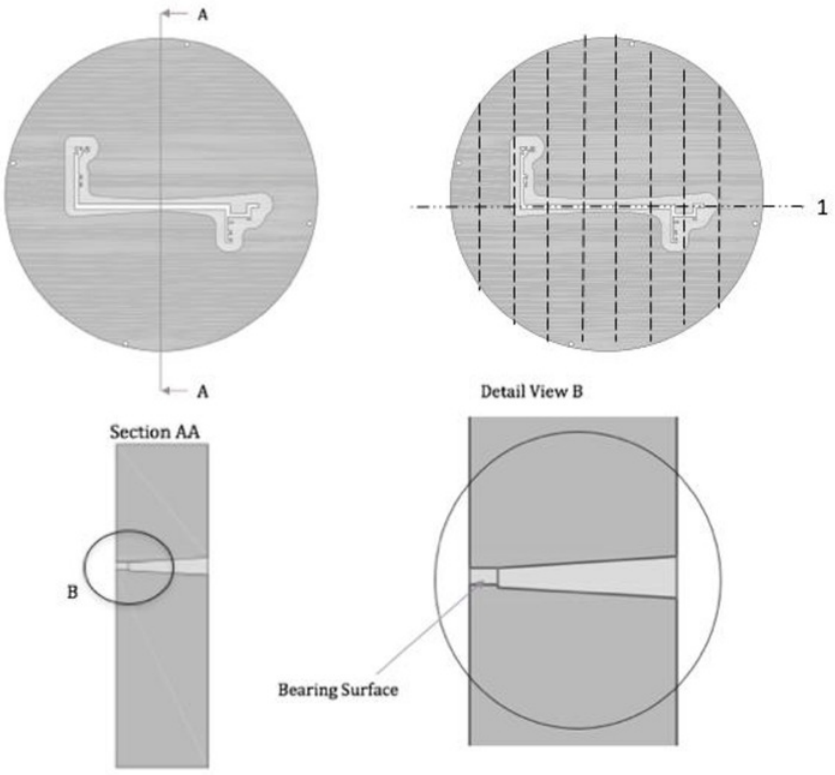

Figure 3 Engineering drawing of die provided by Austex dies sowing section cuts and cross section through it.

Table 4 Sample names and locations in which they were cut from (" Lot 1")

Sample Number	Section cut from Die	Location on Extrusion die
1	9	Bearing surface of die
2	13	Bearing surface edge at corner of die
3	13	Cross section through bearing surface
4	9	Surface of die

Table 5 Sample names and locations in which they were cut from (" Lot 2")

Sample Number	Section cut from Die	Location on Extrusion die
1	3	Bearing surface of die
2	3	Cross section through bearing surface
3	4	Cross section through middle of die
4	4	Surface of die

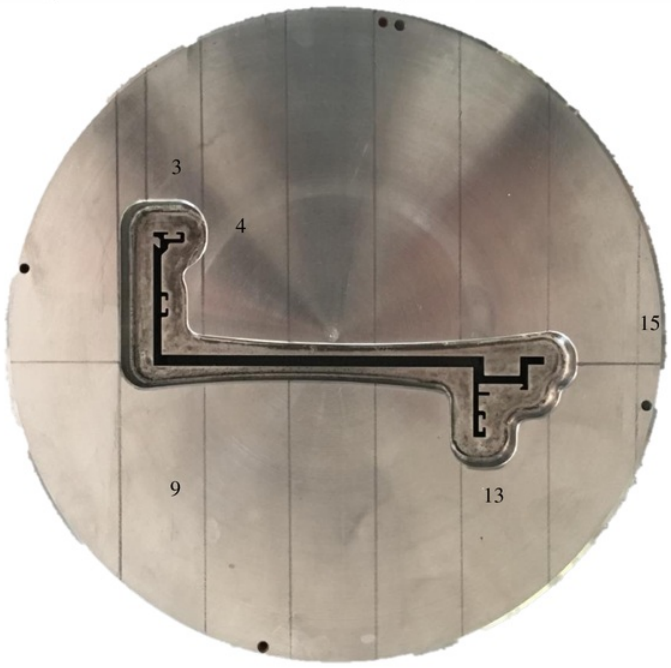

Figure 4 Reference image for sectioning die showing cut location and sample locations.

From here the smaller samples were then placed into a Struers Secotom 50 precision cutter, in order to generate specimens suitable for mounting and polishing.

A Struers ClitoPress-15 mounting machine was then used to mount the samples. Specimens were mounted in a DuroFast thermosetting resin (magnetic), suitable for SEM analysis later on. A pressure of 250 Bar and a temperature of 180°C were used for the mounting process. The final preparation of the samples before examination was grinding and polishing. This took place in a Struers Tegramin. This semiautomatic polishing machine allowed for precise control of polishing compounds in order to ensure best results. The procedure consisted of two grinding steps followed by three polishing steps detailed in Table 6 below.

It should be noted that after the final polishing, it appeared that the samples contained water marks. In an effort to remove these, the final polishing step was repeated and the samples re-cleaned and dried with ethanol. This however still did not remove the marks. It was decided to leave the samples as they were and re-examine them after the etching process, with the idea that once under the microscope we would have a better understanding of what had caused the marks.

Table 6 Grinding and Polishing Procedure for Samples [4].

Grinding		
Step	PG	FG
Surface	MD-Piano 220	MD-Allegro
Abrasive Type		DiaPro Allegro/Largo 9 µm
Lubricant Type	Water	
Speed (rpm)	300	150
Force (N) / Specimen	35	35
Holder direction	>>	>>
Time (min)	01:00	07:00

Polishing			
Step	P 1	P 2	OP
Surface	MD-Dac	MD-Nap	MD-Chem
Abrasive Type	DiaPro Dac 3 µm	DiaPro Nap B 1 µm	OP-AA, 0.02 µm
Lubricant Type			
Speed (rpm)	150	150	150
Force (N) / Specimen	35	30	15
Holder direction	>>	>>	><
Time (min)	06:00	01:00	01:00

3.2 Hardness Testing

To gauge a better understanding of the extent of the heat treatment the dies have already undergone, several samples from various sections of the die were placed on a bench mounted Vickers hardness tester. Hardness is the material's ability to withstand indentation. A Vickers hardness test is an optical measurement method used to assess a material's microhardness. The process is conducted using a diamond indenter in the shape of a right pyramid. It has opposing sides sitting at 136 degrees to each other. A force is then applied to the indenter, and the result is an indentation on the material's surface whose area we can calculate. The Vickers hardness is simply given by the quotient of force and area.

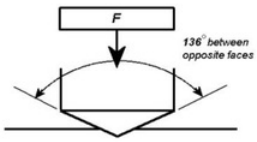

Figure 6 Hardness indenter parameters

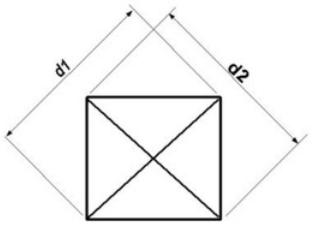

Figure 5 Calculation of area of hardness indent

$$HV = \frac{F(\mathrm{Sin}\left(\frac{136}{2}\right))}{d^2}$$

where:

F is given as the force in Kgf or Newtons.

d is the mean of the two diagonals (d1 and d2).

The following figures detail the results of the initial testing.

Figures 7 and 8 below are the results of two initial hardness tests carried out in accordance to the method described above. The tests were conducted in two very specific locations. Figure 7 shows the test on the bearing surface itself, while figure 8 shows a test conducted on a cross section through the bearing surface. The choice of these test locations was to validate certain details highlighted in my literature review previously.

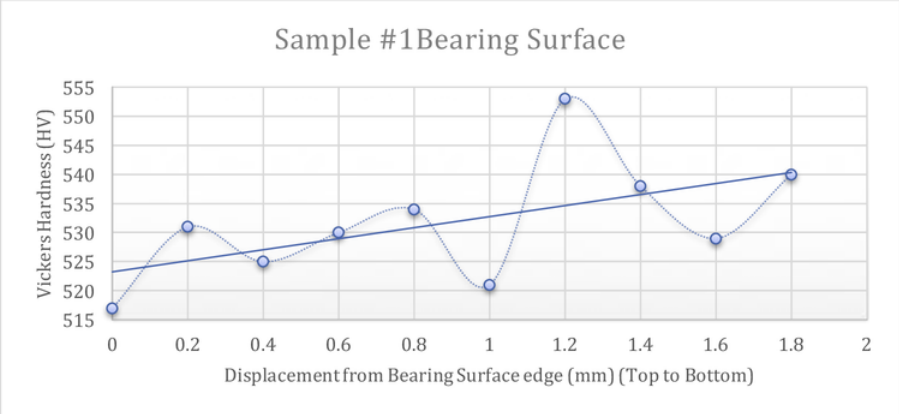

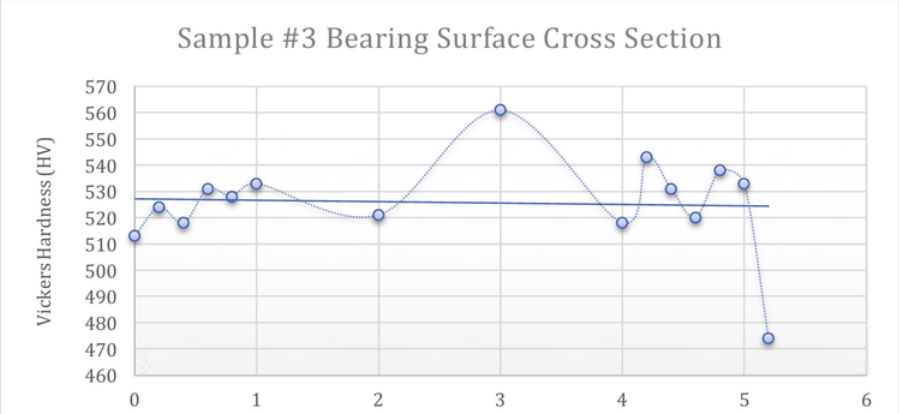

Figure 7 Microhardness test results for sample 1 lot1 bearing surface analysis

While these initial results are far from definitive, they were primarily used to gain a better understanding of the condition of the die and give insight to possible areas that needed further investigation.

In the ideal extrusion process, we would only want the aluminium billet to come into contact with the extrusion die once. This would be on the leading edge of the die's bearing surface. This would lead to an extrusion with minimal friction and perfect surface finish, however in reality the bearing surface varies in depth based on the desired extrusion profile. Whilst it is tapered to avoid excess contact during extrusion, the profile inevitably makes contact at multiple points along the die's bearing surface. The idea of the tests in figures 7 and 8 were to assess exactly this. Figure 7 shows a sample taken from a section of the die's hardened bearing surface. Here I wished to observe if the hardness of the surface increased as we moved further away from the leading edge of the bearing surface. This would be expected as the surface itself is tapered for this reason, to minimise excess contact between the two materials during extrusion. In figure 7 the hardness indents began at the leading edge of the bearing surface and moved away in 200μm increments. Looking at the results we can see that there is a general trend. While not conclusive, it does suggest that this is exactly the case. Further investigation should be made to see if a similar trend is present along the entire bearing surface of the die, particularly at corners where the more intricate geometry of the die causes the extrusion material to naturally flow at a slower rate and hence cause excess wear of the die.

Similarly figure 8 looks at the bearing surface, however rather than examine the face of the surface, it is a cross section taken through the middle of it. Literature such as Björk's work in [7] suggests that it is possible to have a nitrided surface that is too hard. The over hardened surface of the die can become brittle leading to crack propagation and ultimately failure during extrusion. As well as this it can cause the supporting material beneath the surface to become weakened. This is due to the fact that the hardened bearing surface is capable of withstanding the elevated forces and temperatures during extrusion, however the underlying material which is of significantly decreased hardness begins to fail under the pressure and temperature of extrusion.

The aim of the test in figure 8 was to assess the difference in hardness between the bearing surface and the underlying material, looking for vast differences in hardness that could lead to premature wear of the die. As can be seen from the results, whilst I did have several outliers, the overall range of hardness was only 36HV. This result suggests that the difference in hardness is negligible between the bearing surface and underlying material, and suggests that the effects of heat treatment on the die are fairly uniform throughout its cross section.

3.3 Etching The Samples

In order to examine the samples under a microscope they must first be etched. While it is necessary to polish the samples to a mirror finish, a sample that has not been etched can appear as a white plane under a microscope. Etching selectively corrodes certain carbides within the steel. These appear as darker regions when examined and give contrast to the surrounding material. Etching has the ability to reveal faults such as cracks, as well as the shape and size of grain boundaries [30].

Etching tool steels can be difficult due to the large number of alloying elements present. The most common etchant used for high alloy tool steels in Nital.
Nital is a composition of Nitric acid and Ethanol. Solutions of 2-10% are commonly used to reveal microstructure [30]. The time and exact concentration of solution varies, so some trial and error is required to determine the required degree of dullness imparted on the samples. For this reason, three samples were prepared using a 2% Nital solution. The samples were soaked for several minutes and checked regularly. They were removed from the solution when a reasonable finish was achieved. As a point of comparison under the microscope a fourth sample was also prepared, this one etched with a 4% Nital solution. An increased rate of corrosion was observed on this sample as its dull finish surpassed that of the 2% solution quickly. It was left for a further 1-2 minutes before being cleaned with water and ethanol along with the other samples.

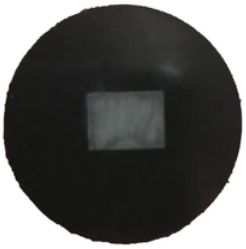

Figure 9 Sample 1 Etched in 2% Nital Solution

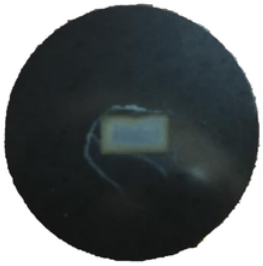

Figure 10 Sample 4 Etched in 4% Nital Solution

3.4 Scanning Electron Microscopy (SEM) And Energy-Dispersive X-Ray Spectroscopy (EDS).

In order to gain the best possible view of the samples, a bench mounted Phenom XL Scanning Electron Microscope was used operating at 10Kv. The aim was to observe features within the microstructure and correlate it to a respective process within the heat treatment process. Alongside this I hoped to observe failures within the microstructure as well as the die's geometry, particularly corners and edges where it is well documented that failures often occur. This was done so that any possible issues could be documented and addressed later.

Further sample analysis in terms of composition and element dispersion mapping were achieved using the same unit, however to achieve this I utilised the Energy-Dispersive X-ray Spectroscopy (EDS) function. The EDS function uses the generated electron beam to remove a k-shell atom from the point it comes into contact with. The removal of this k-shell electron generates a chain reaction. Electrons from outer shells rush to fill the void created by the removal of this electron and this transitioning of electrons between shells generates a characteristic x-ray of a known energy. The SEM has detectors that read these characteristic rays and are hence able to identify an element.

4. RESULTS

The following figures show the results of both SEM and optical light microscopy on samples taken from the die shown in figure 3. After examining the samples an analysis was made do determine the effectiveness of the varying concentrations of etching solutions. SEM Figures 11 and 12 definitively show a difference between the two suggested concentrations.

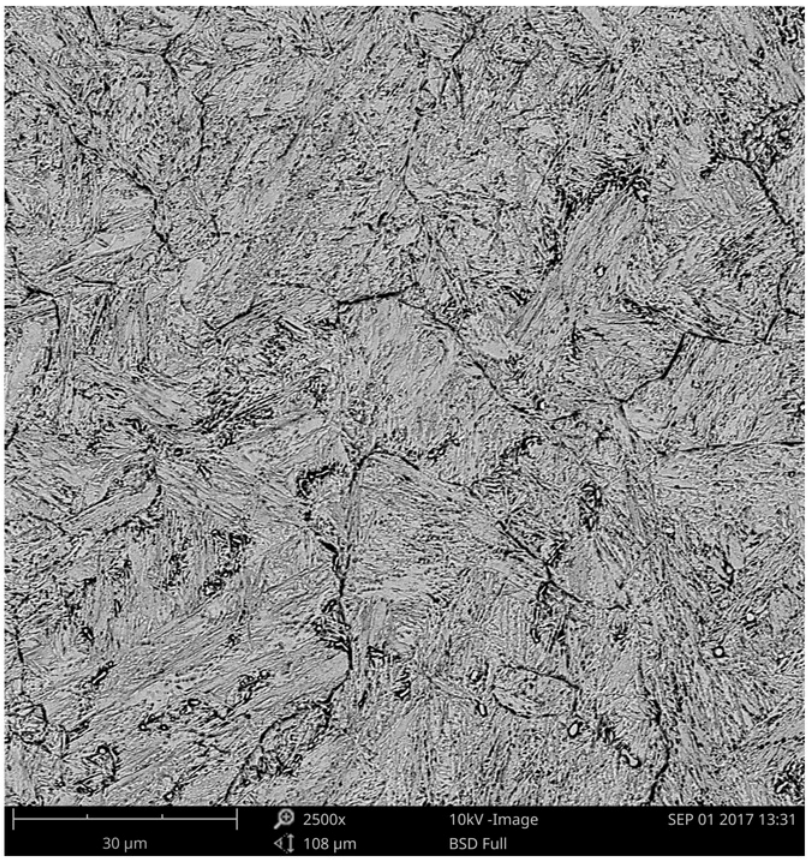

Figure 11 "Sample 1 (Lot1)" Microstructure of bearing surface of the die etched in 2% Nital solution.

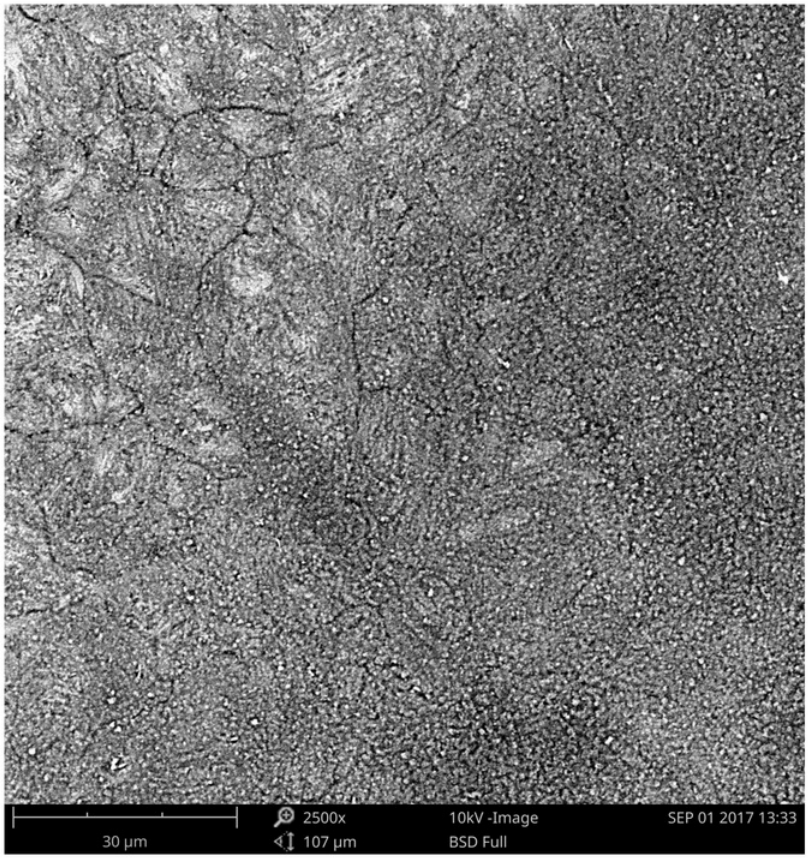

Figure 12 "Sample 4(Lot1)" Microstructure of surface of Die etched in 4% Nital solution.

Both figures 11 and 12 were captured under the same conditions and magnification. While at first it may seem that the appearance of their respective microstructures are different, this is simply a case of sample 4 being over etched. Closer examination of the images reveals a similar grain structure and size of approximately 20-30µm. From this we can say that the 2% Nital solution proved to be better for etching the samples as shown by the results in figure 11. The 2% solution allowed me to clearly identify grain boundaries, as well as ferrite and cementite layers within the die's microstructure. These figures further demonstrate the die's consistent nature as found through the initial hardness testing results in figures 7 and 8.

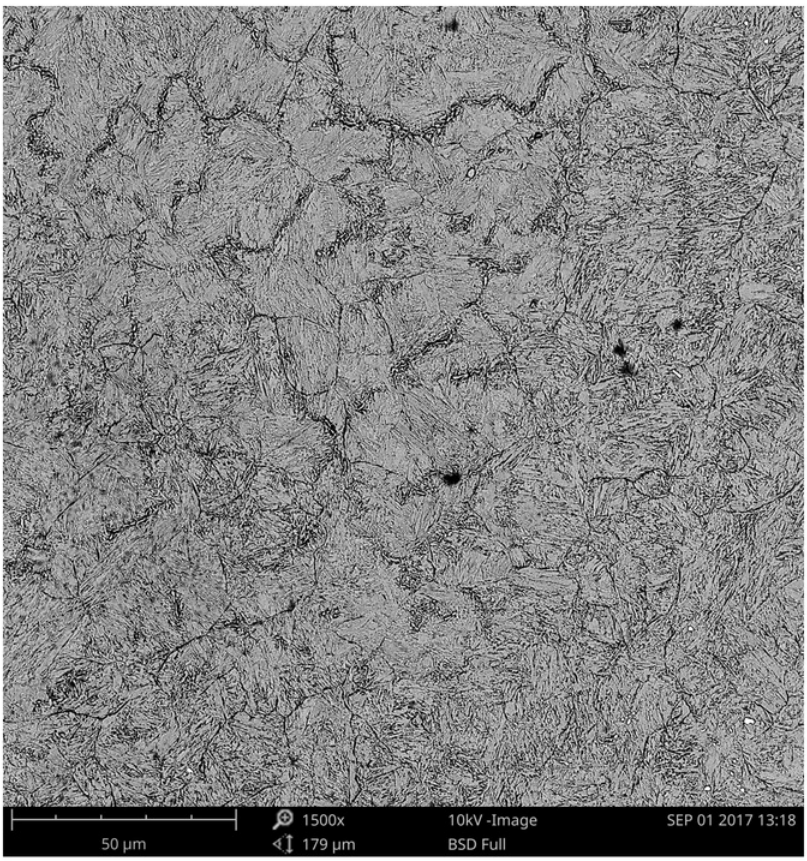

Figure 13 "Sample 2 (Lot1)" Microstructure behind leading edge of bearing surface at a corner.

Here we see a pearlite (layered ferrite and cementite) microstructure and consistent grain size throughout. A perlite microstructure is only achieved under specialised heat treatment conditions, which is why the process must be closely controlled. The layering of ferrite and cementite within a perlite microstructure is responsible for its characterisation as hard and strong, and is also what gives it good wear resistance.

Figure 14 below is again an image of the microstructure of the bearing surface. This image looks at a particular corner of the die. Research suggests that tight corners on extrusion dies can present problems with increased friction, subsequently leading to premature wear. Hence it was decided to specifically analyse such geometry within the die as it was most likely to result in a failure. The corner shown in figures 14-15 is supposed to produce a profile of 90° however it is clearly evident that sufficient amounts of material have worn away

during the extrusion process. The magnified view shown in figure 14 clearly shows evidence of cracks, as well as pitting of the material from the bearing surface. I used the discovery of this failure as the starting point of my analysis in order to determine what caused the failure and how it could be prevented or delayed.

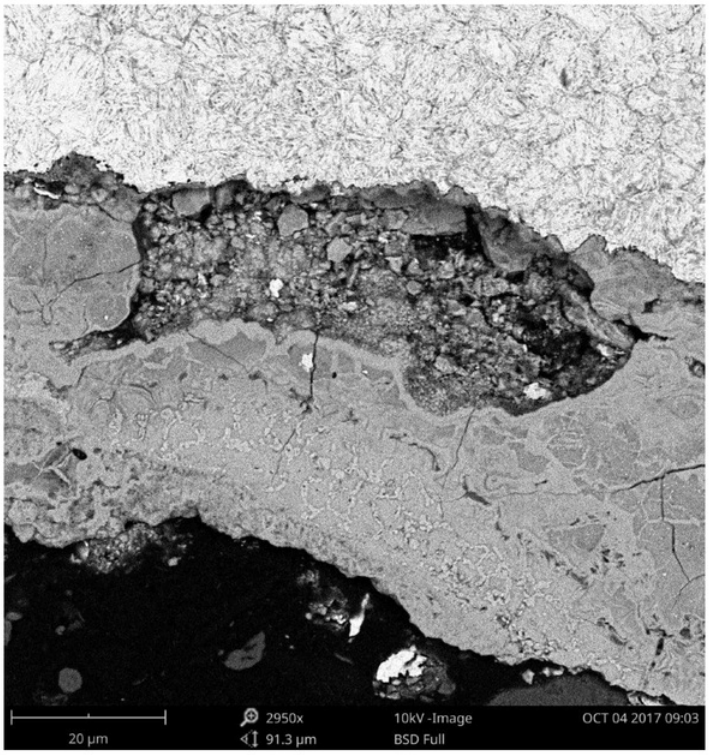

Figure 15 "Sample 2(Lot1)" Bearing surface at corner of die.

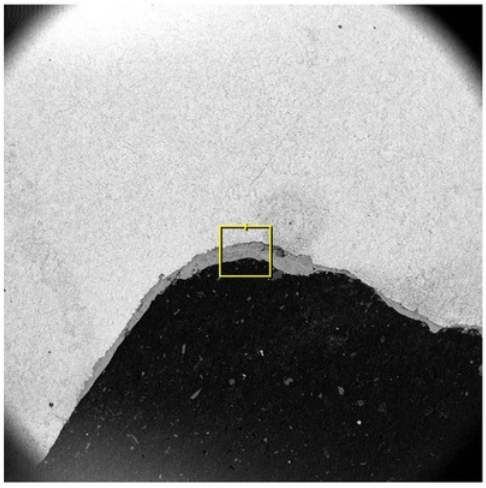

Figure 14 Reference image for figure 14

Clearly figure 14 shows an area in which the die has suffered significant degradation. As previously mentioned, it is well documented that a die's geometry plays a significant role in its longevity. We know a more intricate geometry leads to a greater extrusion force, in turn wearing the die quicker. It is therefore expected, as in the case of sample 2, when looking at a corner section of the die we would expect to see greater amounts of wear.

Further analysis of the sample using EDS revealed the extent of the damage allowing me to see exactly what was there and what had worn away.

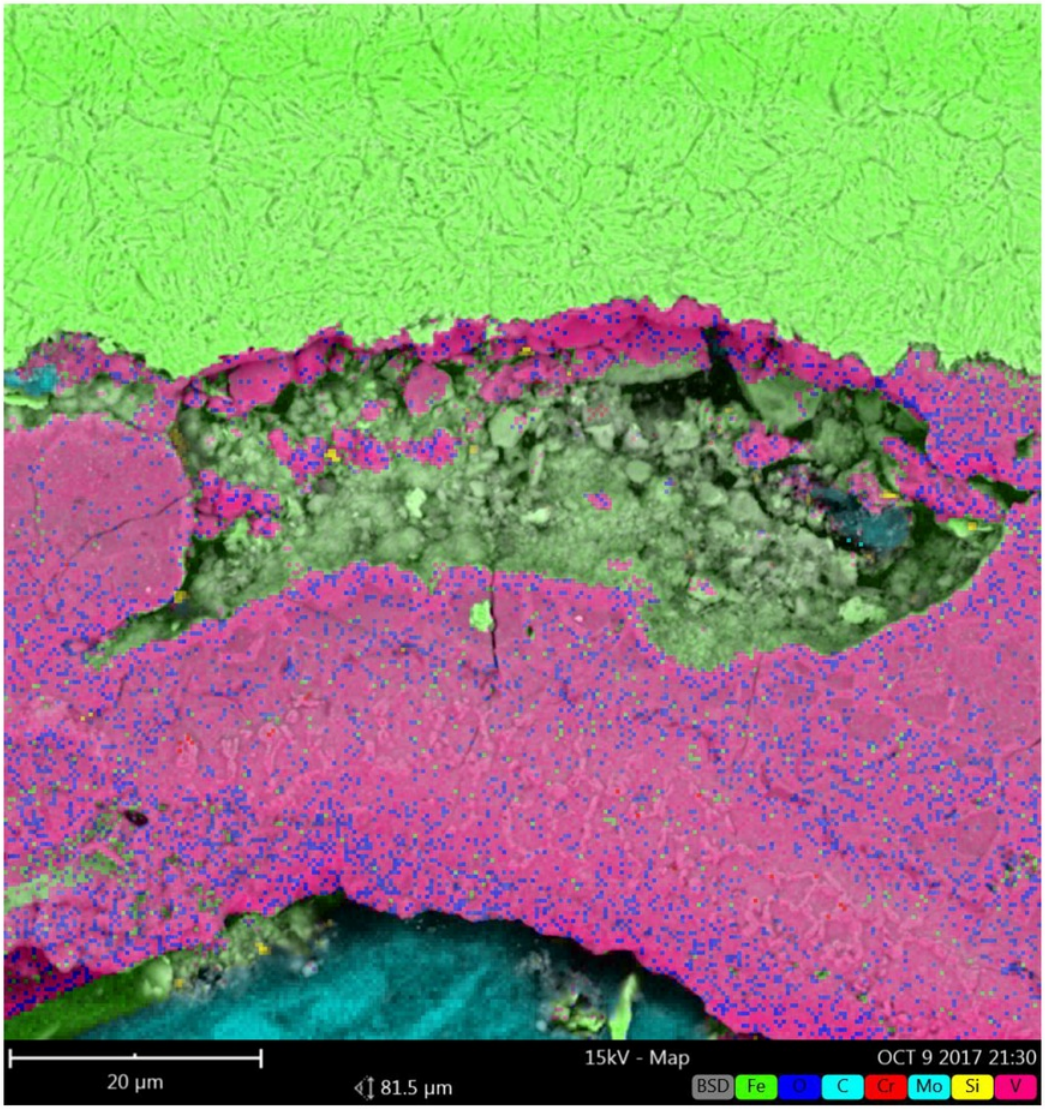

Figure 16 EDS Mapping of "Sample 2 (Lot1)"

Initially when looking at figure 16 we see an interesting result. There is a clear division on the sample, almost as though we are looking at different phases within the microstructure. However, from the previous results we know that this is not the case and the die has a consistent perlite microstructure. The combined map shows all of the elements we would expect to see within the sample with the exception of nitrogen. Given that this is taken from the bearing surface of the die we would definitely expect to see some nitrogen here as a result of the nitriding process. Also from table7 below we know there should be some nitrogen present.

Table 7 EDS composition analysis "Sample 2 (Lot1)"

Element Number	Element Symbol	Element Name	Atomic Conc.	Weight Conc.
8	O	Oxygen	37.38	23.12
6	C	Carbon	29.12	13.52
26	Fe	Iron	24.04	51.89
7	N	Nitrogen	4.86	2.63
24	Cr	Chromium	2.18	4.39
14	Si	Silicon	1.43	1.55
42	Mo	Molybdenum	0.55	2.05
23	V	Vanadium	0.44	0.85

To better understand why it does not show on the map we examined the EDS Spectrum data shown below.

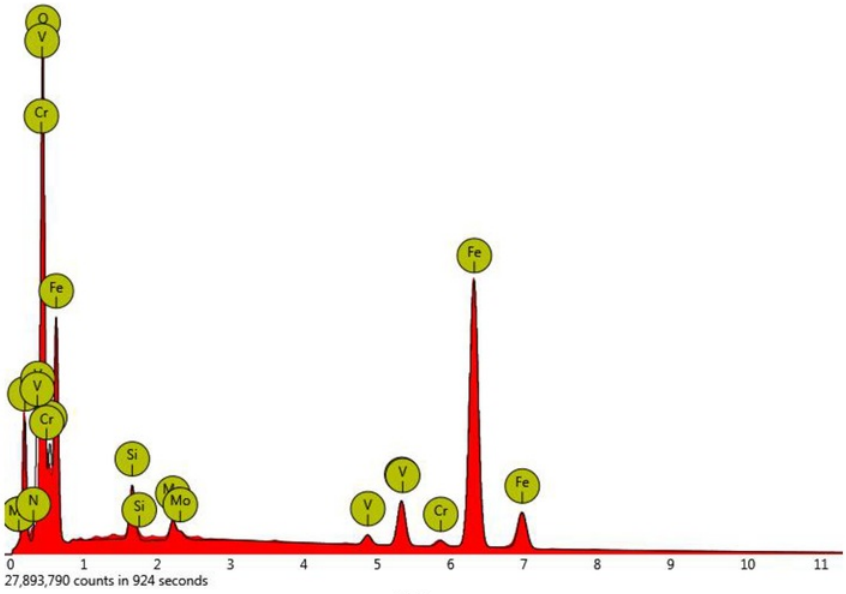

From figure 17 we can see that the nitrogen peak lies close to the left-hand side of the graph. These peaks are indicative of weaker readings. Also, notice the peaks for nitrogen and vanadium overlap at this point. Vanadium being the heavier element of the two has a greater number of electron shells available, hence will give a spectrum with more peaks. This is the case in figure 17, where we can see four vanadium peaks as opposed to nitrogen's one. The vanadium peaks spread further to the right of the graph, indicative of a stronger energy reading. This is why it shows as the more predominant of the two elements on the mapping image, although by weight concentration it is far less. Figure 18 below shows the results for the same sample when the other elements from the EDS spectra graph have been disabled.

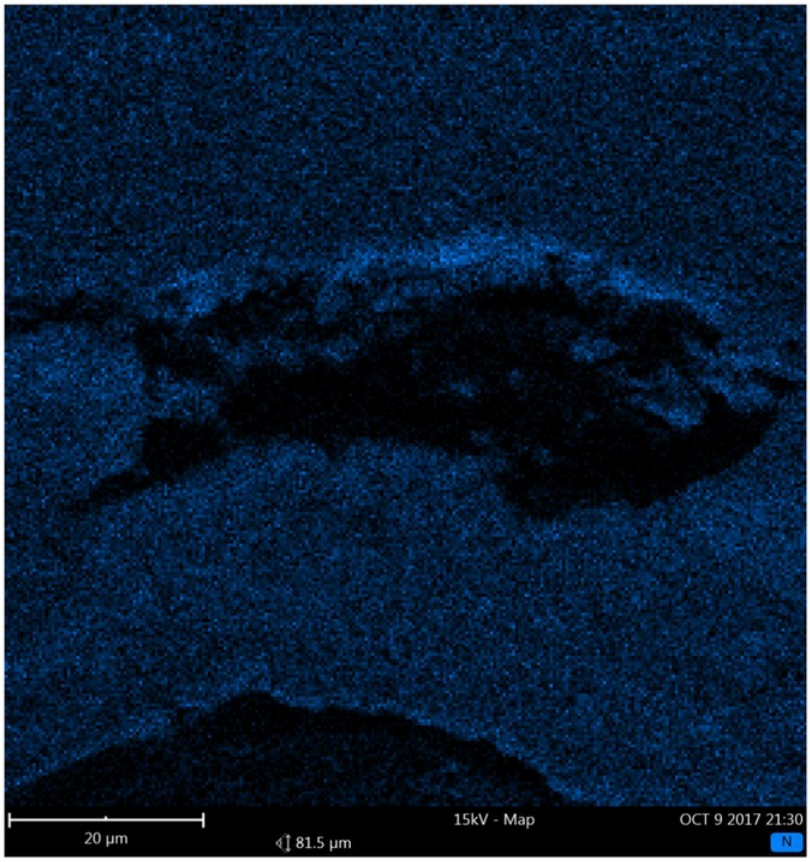

Figure 18 Nitrogen dispersion through sample 2

When looking at figure 18 we do see the expected nitrogen dispersion throughout the sample, however it is clear that the nitride layer has simply worn away. The brighter region in the foreground is the bearing surface. Its brighter appearance is due to a stronger nitrogen reading. This is to be expected because it is the exposed surface during the nitriding process. Looking further back in the image we see the darker region where the die has clearly degraded and a significant portion of the surface is missing. Here we see no nitrogen. Further behind this we see a slight colour variance where the background region seems to be a lighter blue. This lighter region is the diffusion zone as described earlier.

After examining a failure on the bearing surface of the die I turned my attention to other regions for examination. Figures 19 and 20 both look at the microstructure of the surface of the die. The scale represents a distance of 5μm. Unlike the earlier figures, both images show a difference in microstructure not seen previously in any of the other samples. The white regions within the microstructure, as highlighted, appear to potentially be significantly harder regions within the material. This is detailed by the increased molybdenum present in the composition analysis in tables 8 &9.

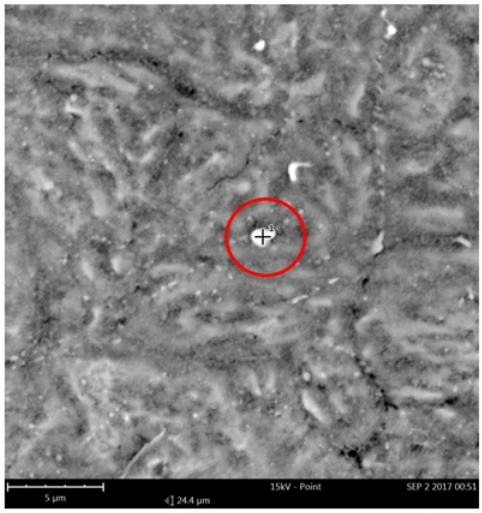

Figure 19 Sample 4 Microstructure composition analysis "Spot 1"

Table 8 EDS "Spot 1" Composition red highlighted region

Element Number	Element Symbol	Element Name	Atomic Conc.	Weight Conc.
8	O	Oxygen	32.08	15.70
6	C	Carbon	28.10	10.32
26	Fe	Iron	15.97	27.29
42	Mo	Molybdenum	10.74	31.54
7	N	Nitrogen	4.25	1.82
14	Si	Silicon	2.96	2.54
24	Cr	Chromium	2.63	4.18
23	V	Vanadium	1.97	3.07
38	Sr	Strontium	1.05	2.82

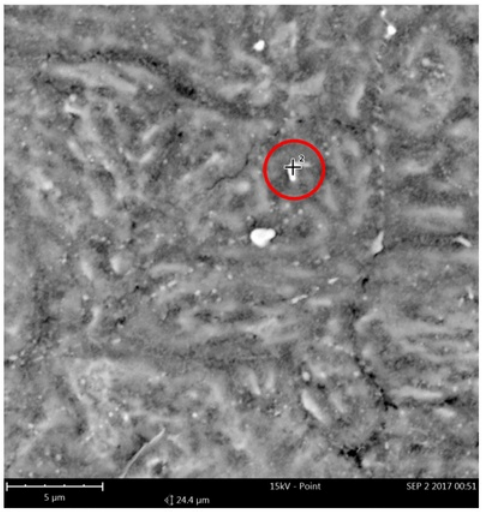

Figure 20 Sample 4 Microstructure composition analysis "Spot 2"

Table 9 EDS "Spot 2" Composition red highlighted region

Element Number	Element Symbol	Element Name	Atomic Conc.	Weight Conc.
8	O	Oxygen	39.61	23.43
6	C	Carbon	27.82	12.35
26	Fe	Iron	16.63	34.33
7	N	Nitrogen	5.14	2.66
42	Mo	Molybdenum	4.62	16.40
24	Cr	Chromium	2.79	5.36
14	Si	Silicon	1.82	1.89
23	V	Vanadium	1.11	2.08

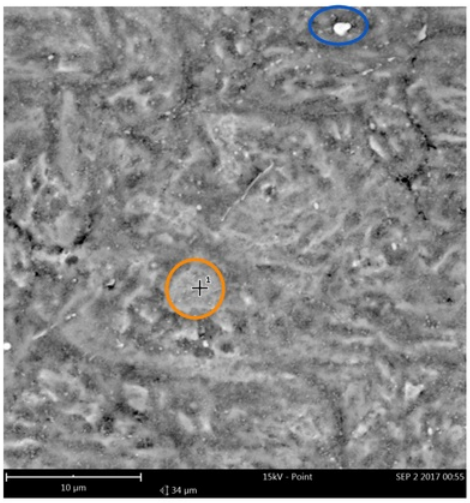

Figure 21 Microstructure composition analysis comparison between various regions on dies surface.

Table 10 EDS "Spot 3" Composition analysis orange highlighted region

Element Number	Element Symbol	Element Name	Atomic Conc.	Weight Conc.
26	Fe	Iron	45.81	72.06
8	O	Oxygen	28.13	12.68
6	C	Carbon	20.32	6.87
24	Cr	Chromium	3.24	4.74
14	Si	Silicon	1.28	1.01
42	Mo	Molybdenum	0.70	1.88
23	V	Vanadium	0.53	0.76

Figure 21 above gives insight into the effects of extrusion and degradation of the die. The figure is a comparison of a point highlighted in orange to that of the blue region of increased molybdenum. Graphing the results as shown in figure 22 below, highlights the variances in weight composition of several of the alloying elements within the steel die. The compositions for each of the columns were taken from the same sample (Sample 4 – Surface of the Die). The blue and orange columns correlate to the two points highlighted in figure 21 above. It was noted that there was a difference in composition between the two spots in figures 19 and 20, hence an average was taken for the comparison.

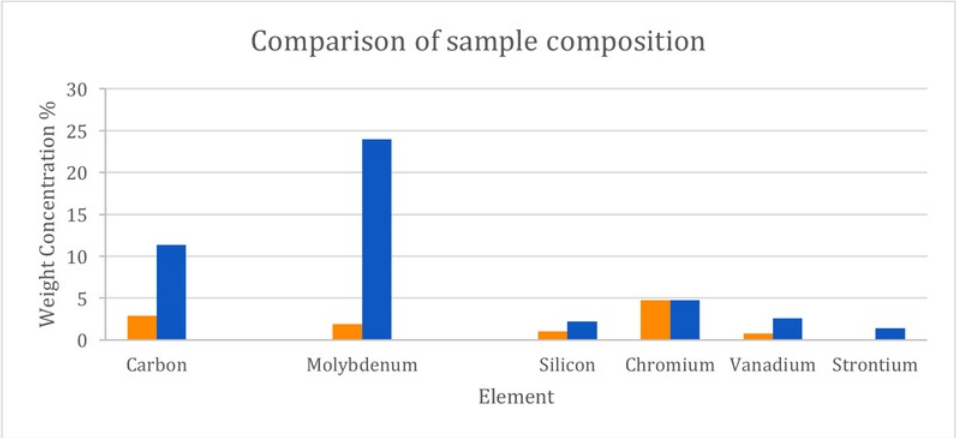

Figure 22 Composition analysis comparison for points shown in figure 21.

Looking at the results in figure 22 we can clearly see that the points marked in figures 19 and 20 have significantly higher concentrations of molybdenum and oxygen indicating the possible presence of molybdenum oxide. These higher concentrations are indicative of regions of significantly harder material within the steels microstructure, and have considerable potential to distort the crystalline lattice, in turn compromising the material.
While it appears that there is also a considerable variance in carbon percentage by weight as well, it should be noted that organic elements such as carbon are notoriously difficult to measure accurately through the use of EDS. Consequently variances such as those above in figure 22 are deemed irrelevant.

Up until this point the presence of molybdenum spots have only occurred on samples cut from the face surface of the die where it comes into contact with the aluminium billet during extrusion. To assess the extent of these occurrences, a larger sample was cut from the surface of the die for examination. The sample shown in figure 23 below was taken from the side of the die. In doing this I ensured that it did not come into contact with the aluminium during extrusion so I could rule out chemical interactions as the cause for oxidation. The cut sample was still exposed to the same nitride treatment process as the rest of the die and any temperature variances that would lead to oxidation, could only be the result of thermal transfer during extrusion. In doing this I could compare it to the previous samples in figures 19 and 20.

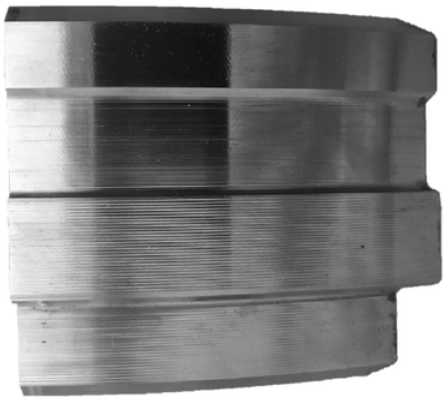

Figure 23 Sample cut from surface of die (Section 15 see figure 4)

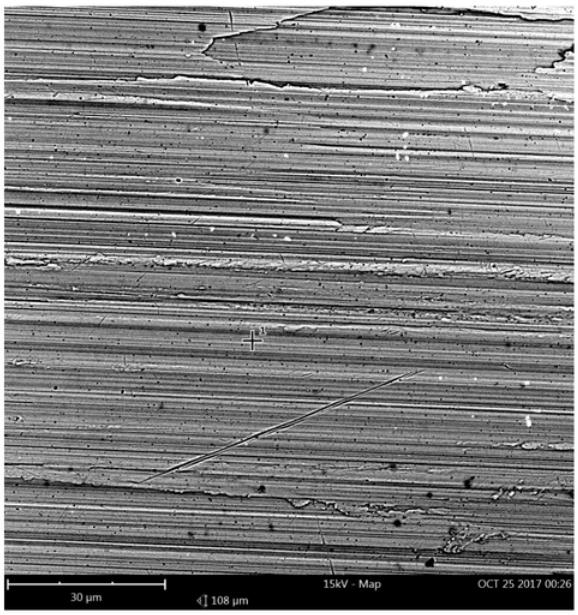

Figure 24 SEM image sample shown in figure 20 (30 Micron Scale)

Table 11 EDS composition of sample shown in figure 20

Element Number	Element Symbol	Element Name	Atomic Conc.	Weight Conc.
26	Fe	Iron	83.93	89.60
24	Cr	Chromium	4.89	4.86
7	N	Nitrogen	7.48	2.00
42	Mo	Molybdenum	0.90	1.66
14	Si	Silicon	1.97	1.06
23	V	Vanadium	0.57	0.55
25	Mn	Manganese	0.26	0.27

When examining the sample shown in figures 24 and 25, we again see regions of white dots. Although this appears to be contamination on the surface of the die, the following figure disproves this and confirms the findings in figures 19 and 20 that these are indeed molybdenum concentrations.

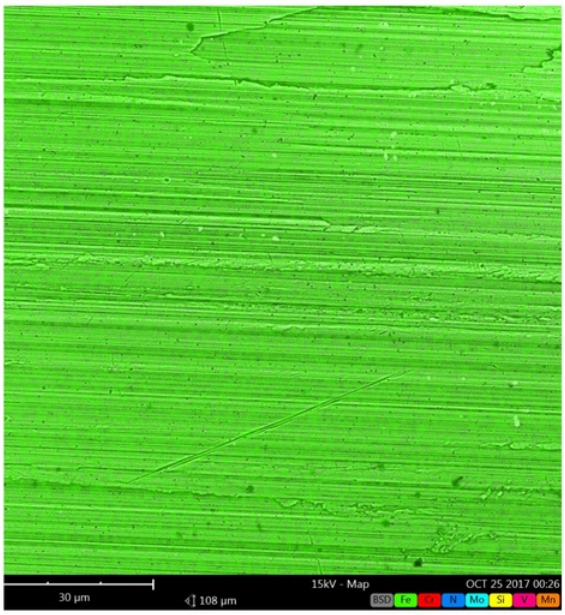

Figure 25 Combined EDS mapping of sample show in figure 20

Table 12 EDS Composition analysis for sample show in figure 24 (Average element concentration over map)

Element Number	Element Symbol	Element Name	Atomic Conc.	Weight Conc.
26	Fe	Iron	83.93	89.60
24	Cr	Chromium	4.89	4.86
7	N	Nitrogen	7.48	2.00
42	Mo	Molybdenum	0.90	1.66
14	Si	Silicon	1.97	1.06
23	V	Vanadium	0.57	0.55
25	Mn	Manganese	0.26	0.27

As we can see from figure 25 the material is homogeneous, hence it is difficult to identify one element in particular over the whole map. Selecting the desired elements individually as shown in figure 26 below enables us to see the exact distribution of each throughout the sample.

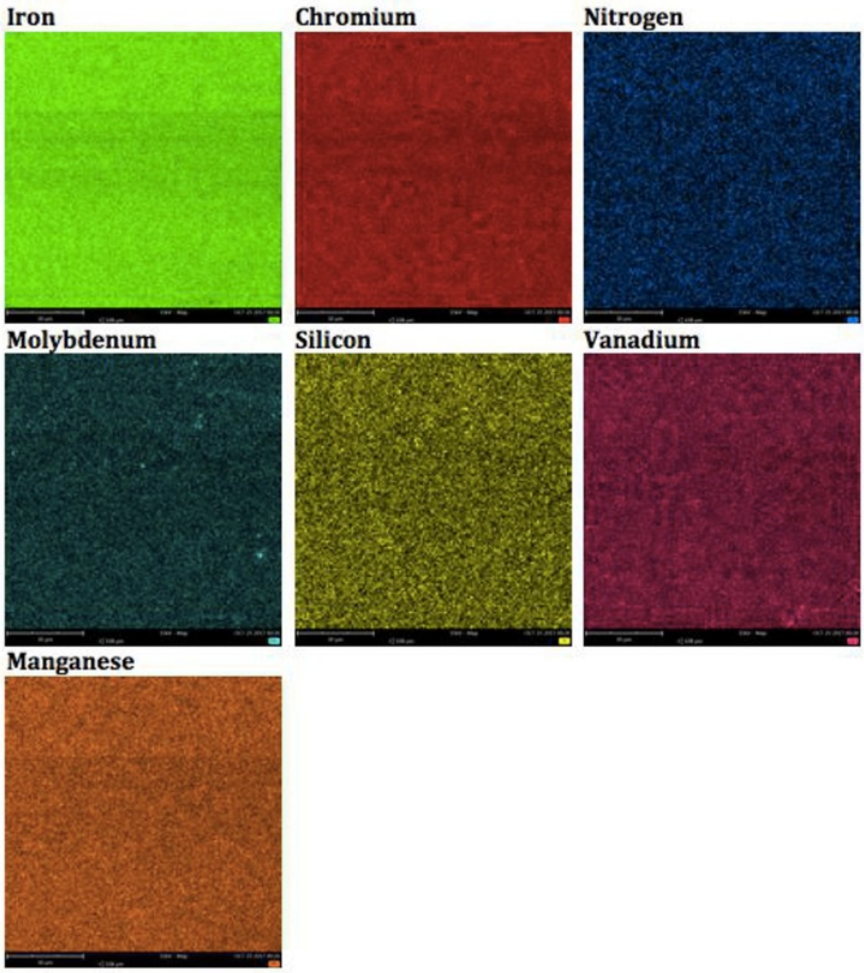

Figure 26 EDS Composition analysis of element distribution from sample show in figure 20

Note that when looking at the map layer showing only the molybdenum we again see brighter regions. These correlate to the exact same spots shown in figures 24 and 25, confirming the findings previously in figures 19 and 20 that these are in fact regions on the die's surface that have significantly higher concentrations of molybdenum.

This means that these areas have a high likelihood of having different mechanical properties when compared to surrounding regions in terms of increased hardness and subsequently brittleness. Also based off the sample location selection we can confirm that the presence of aluminium during extrusion was not the case, and the observed oxidation is in fact caused by transfer of thermal energy throughout the die.

For further examination of the die a second lot of samples were cut. To ensure reliability within the results a secondary lot of specimens (Lot2) were cut from similar regions of the die (i.e. bearing surface, cross section and die surface). The samples were then examined under a light microscope to ensure they did in fact have a similar microstructure to that already observed in first lot of samples.

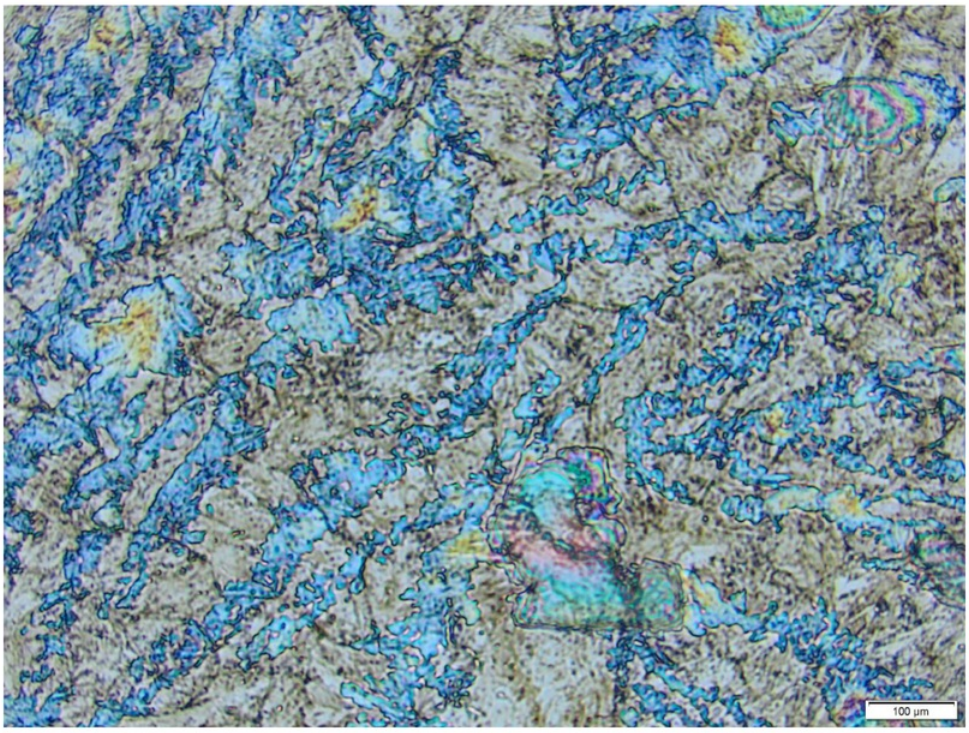

Figure 27 Pearlite microstructure evident in "sample1(Lot2)" taken from bearing surface of die

Figure 27 was an image captured using a light microscope. It was used to ensure that the second lot of samples cut from the opposite side of the die had a similar microstructure, meaning that they were in fact comparable to the first lot of samples.

Note the colour variances in figure 27. We see darker regions and lighter ones. These are the two phases of a perlite microstructure (ferrite and cementite) and this confirms a consistent microstructure and means a comparison between samples is valid.

The Following figures are the results from a series of microhardness tests conducted in a similar manner to that for the first lot of samples. The first figure (28) shows a microhardness test conducted on sample 1 from lot 2. It was conducted in the exact same manner as sample 1 from the first lot of samples (bearing surface top town). The only difference being that like the rest of the samples in lot 2 it was taken from a different region of the die. Note also, 40 sample test points were used this time to give a more definitive overview as to what the hardness profile of the bearing surface is. The second figure (29) is a microhardness test conducted on the sample shown in figure 23 that was cut from the side of the die. It was used as a comparison because this section of the die, in theory, should have remained unaffected from the extrusion process.

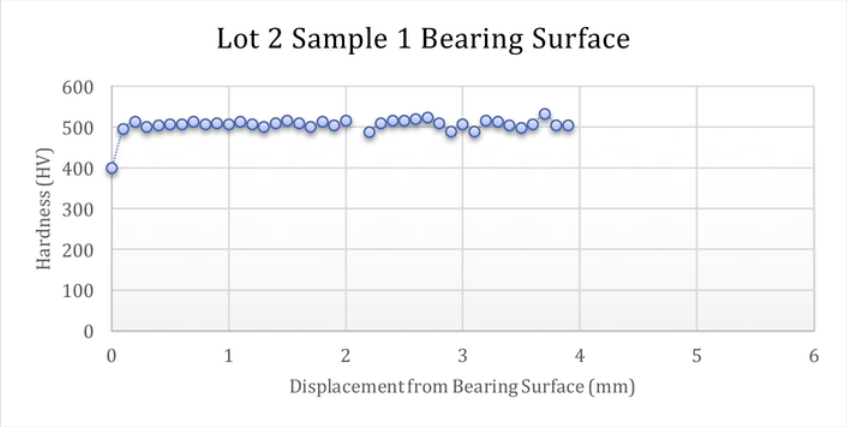

Figure 28 Hardness results sample 1 lot 2 bearing surface analysis.

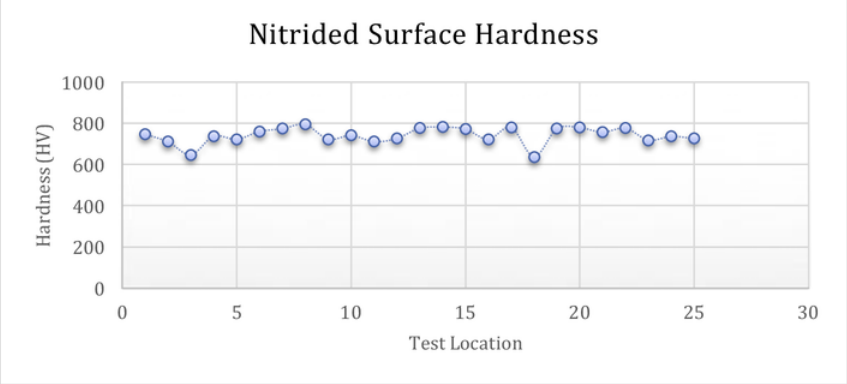

Figure 29 Hardness test results for comparison of nitrided surface and underlying material

Examination of figures 28 and 29 depicts a clear trend that has become visible throughout my investigation of the die. We can see figure 28 looks at the bearing surface of the die. We see a consistent microhardness of between 500 and 550 HV. We do not see an increase in hardness as we would expect from the tapered surface meaning that the contact during extrusion is relatively uniform along the entire surface rather than simply along the leading edge. Comparing this to figure 29 which is a microhardness test of the sample shown in figure 23, we see an average hardness of between 700 and 800HV. The 200HV difference is extremely significant and can only be attributed to a lack of the nitride layer on sample 1 as opposed to that from the sample cut from the side surface of the die.

The following 4 figures were captured using the SEM. Each is an examination of the bearing surface as depicted in sample 1 lot 2 (figure 28). The images were used as definitive proof that the nitride layer has simply been removed and we are now seeing clear degradation of the die's bearing surface as a result of extrusion.

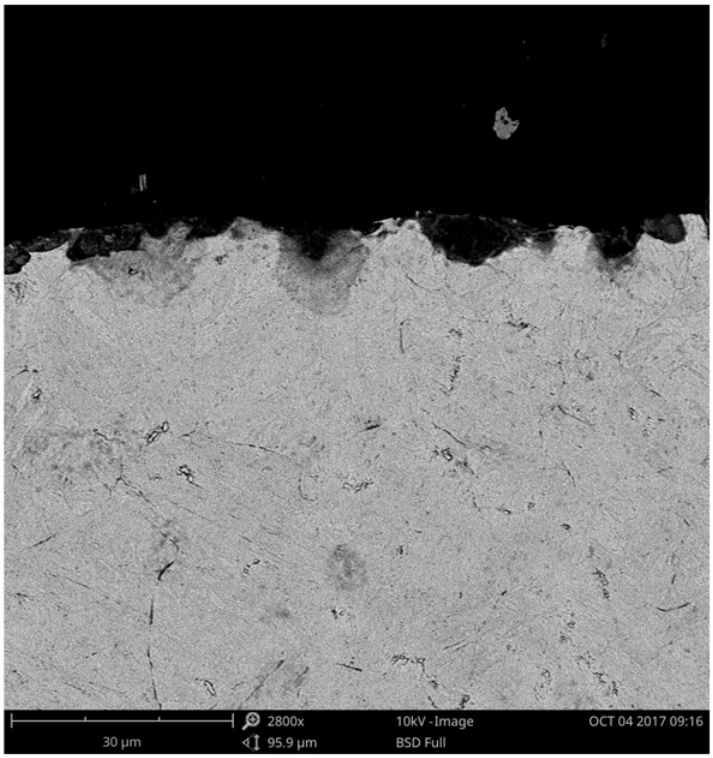

Figure 30 Sample 1 location 2 bearing surface (Lot2

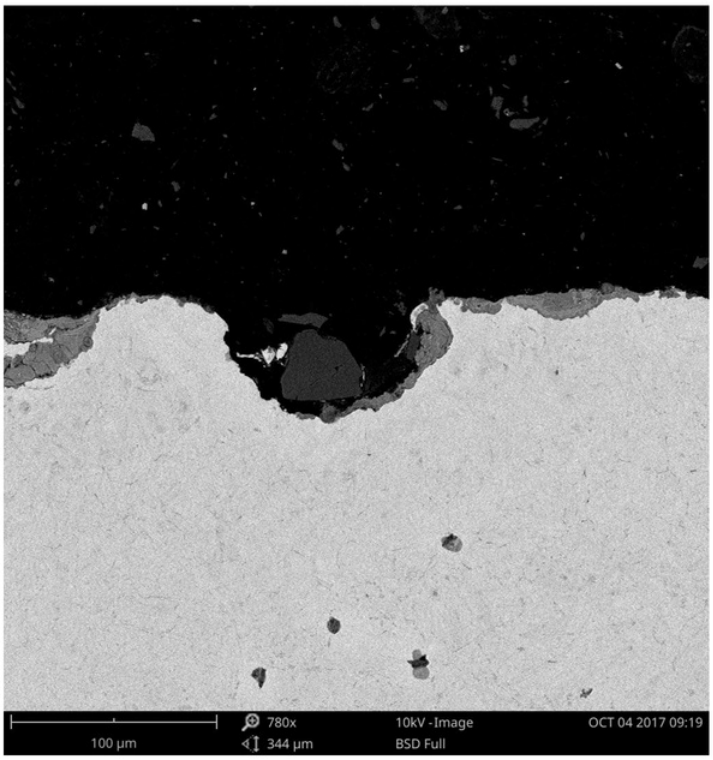

Figure 31 Sample 1location 1 bearing surface (Lot2)

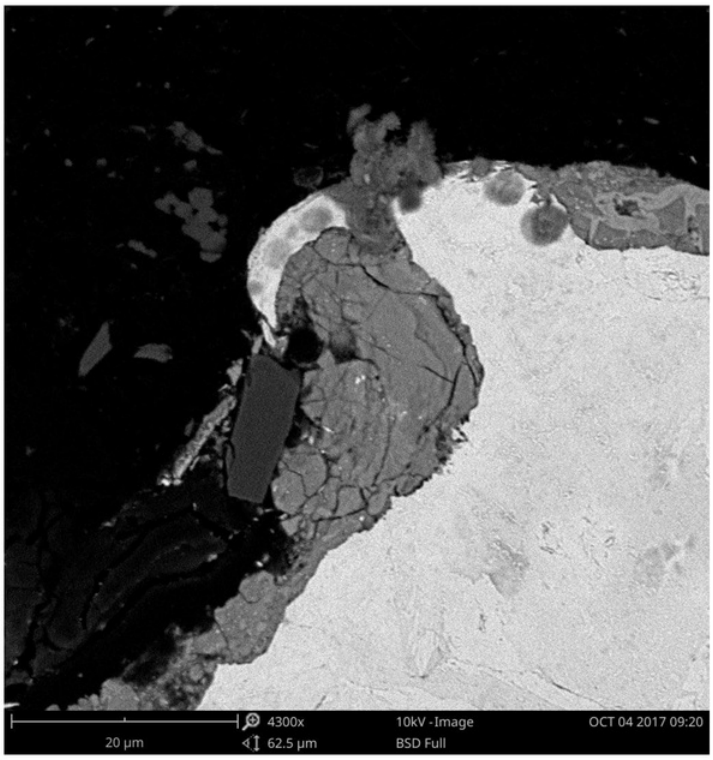

Figure 32 Sample 1 location 3 bearing surface (Lot2)

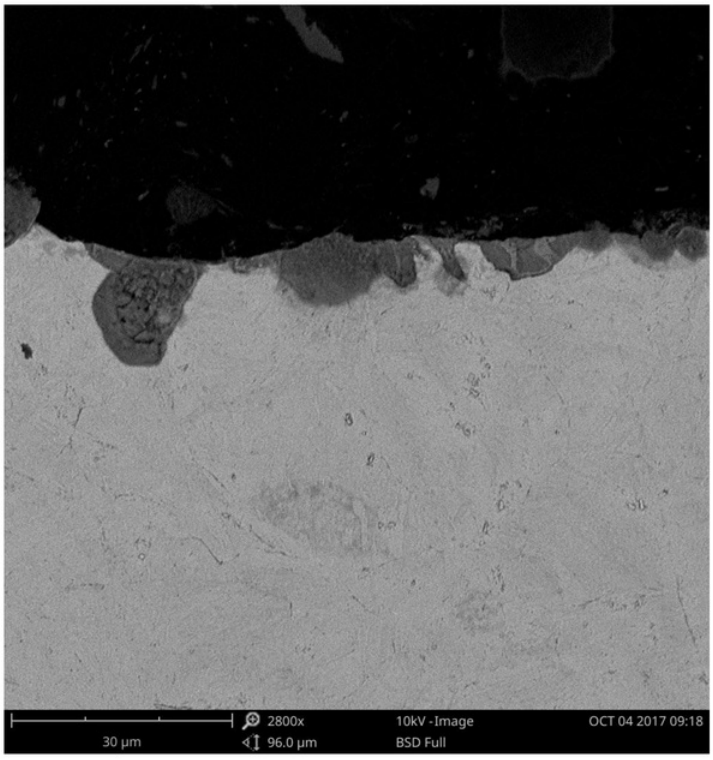

Figure 33 Sample 1 location 4 bearing surface (Lot2)

5. DISCUSSION

It became evident through the testing and analysis of the dies that their microstructure was highly consistent and well within the specified state, as can be seen from the discussion that follows. This observation led me to believe that the heat treatment procedure used to impart the microstructure was sufficient, and any noticeable improvements would be in the quality of the protective surface coating. Moving forward with the project and developing better wearing dies it was decided that focus needed to be given to the monitoring of the nitride layer protecting the die during extrusion. This conclusion was drawn as all examined failures of the die were observed to be a result of the wearing of the nitride layer and subsequently the bearing surface.

Looking at the microhardness results from the hardness tests in figures 7 and 8, and comparing that to the known data provided by Austex Dies, we expect after the dies undergo the specified heat treatment process they emerge with an expected hardness of between 46 – 48 HRC. With that the denotation HRC implies that Rockwell test C was used. Equating this to the Vickers scale used for testing in the labs, we would expect to see a HV between 458 – 490. The results in figures 7 and 8 show the majority of values either lie within this range or exceed it, meaning that the heat treatment method described in table 3 produces dies with a consistent microhardness.

This observation however is not one we would necessarily expect, as the numbers quoted by Austex are hardness pre-surface treatment (nitriding) and the tested results are from a die that has had various surface treatments over its service life. We know the test die was subjected to various nitriding treatments over its lifespan, so to see such minimal variation in hardness is unexpected. This implies that the majority of the nitride layer has been removed.

The results however do enable us to see several other key points. Firstly figure 7 is a hardness test running from the top of the bearing surface down. As mentioned, this is a tapered edge on the die and we would expect to see the hardness increase the further away we moved from the bearing surface. This is due to that fact that in theory the extrusion material should come into contact with it less frequently, and with a decreased force. Figure 7 does show this to some extent, however the 23HV difference observed between the leading and trailing edge of the bearing surface is not as significant as we would expect to see. From this I see further justification that the surface treatment on the die can be considered worn out. Figure 21 further supports this argument, showing that there is almost no difference in hardness along the bearing surface of the die.

Taking the results from figures 7 and 21 and comparing them to those in figure 8, we can see a comparison between the bearing surface of the die and a cross section through it. The cross section is a representation of the underlying material beneath the bearing surface. In accordance with figure 2 in the literature review, when conducting the hardness testing assessing the nitriding case depth, we would expect to see the "total case depth". This is the point at which the hardness drops and the remainder of the materials are fairly uniform in hardness. Figure 8 however shows similar trends to that in figures 7 and 21, meaning that all the points lie within the quoted region for a material that has not been surface hardened. This further suggests that the reason for degradation for this particular die was due to the excessive wearing of the protective nitriding surface layer.

As above, the "total case depth" was never observed in any of the three tested samples, leading me to believe that the nitride hardened layer simply isn't there and has worn away during extrusion. This point is confirmed when looking at figures 30 – 34 where we observe significant portions of the bearing surface have worn away.

The results in figures 7, 8 and 21 do have outliers where there are regions that are noticeably harder than the surrounding material. However, the only figure in which we would expect to see the boundary between the nitrided surface layer and the substrate material is figure 8. Although there is a point on the graph representing a harder surface region, this can in no way be seen as the boundary between the nitrided surface layer and the H13 tool steel. This is due to its location. Taking this point as the total case depth would imply a nitride layer of 1.3mm thickness on a die that has already had an extended service life. The point if far more likely to be attributed to inconsistencies in the nitriding application or variances in the microstructure between the 200-micron test increments. This has already been shown in a review of literature previously and by looking at figures 19 - 20 and the corresponding data in tables 8 – 10.

In order to definitively confirm that the main reason for degradation of the die was lack of a protective surface treatment, I conducted another hardness test as depicted in figure 29. Here I assessed the microhardness of the surface of the die. This region however never comes into contact with the aluminium during the extrusion process. By doing this I hoped to see an area of the die with its nitride layer still intact therefore allowing a point of comparison.

As can be seen from figure 29, the average hardness test yielded a result of 741.48HV as compared to the results in figure 28, where the average hardness was 505.18HV. This is extremely significant as it shows a 32% reduction in material hardness between the nitrided surface layer and the substrate material.

When examining samples cut from the surface of the die using Energy Dispersive X-Ray Spectroscopy (EDS), almost all of the samples displayed white regions. The composition analysis suggested that these areas were molybdenum concentrations. As we know the main purpose for alloying of molybdenum within the steel is to increase its hardness, if a hardness test point fell within one of these regions an increase in hardness would be expected.
The observed molybdenum concentrations appeared from samples of the die cut from its surface. The presence of the molybdenum as shown in figure 22 suggests

that certain areas of the die contain a 20% increase in molybdenum when compared to surrounding regions. These areas are likely to be regions of molybdenum oxide as indicated by composition in tables 8 and 9. It is likely formed during the extrusion process as oxidation of molybdenum only begins to occur above 400°C, with strong oxidation occurring above 600°C [31]. These noted points have the potential to significantly distort the crystal lattice of the metal and the mechanical properties at these specific points would be significantly different to those of the surrounding areas.

When observing the die, I found many cases similar to those shown in figures [34 – 35] below.

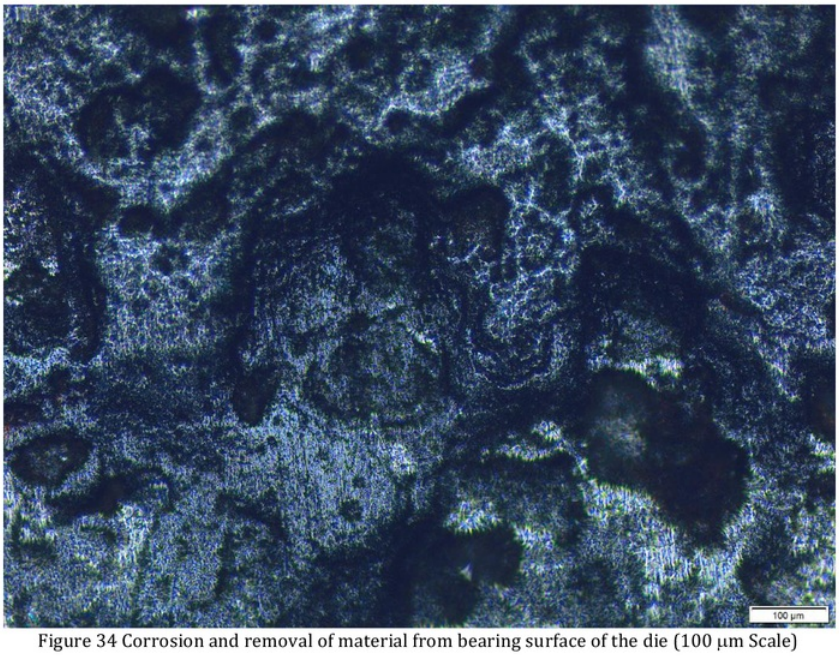

Figure 34 Corrosion and removal of material from bearing surface of the die (100 µm Scale)

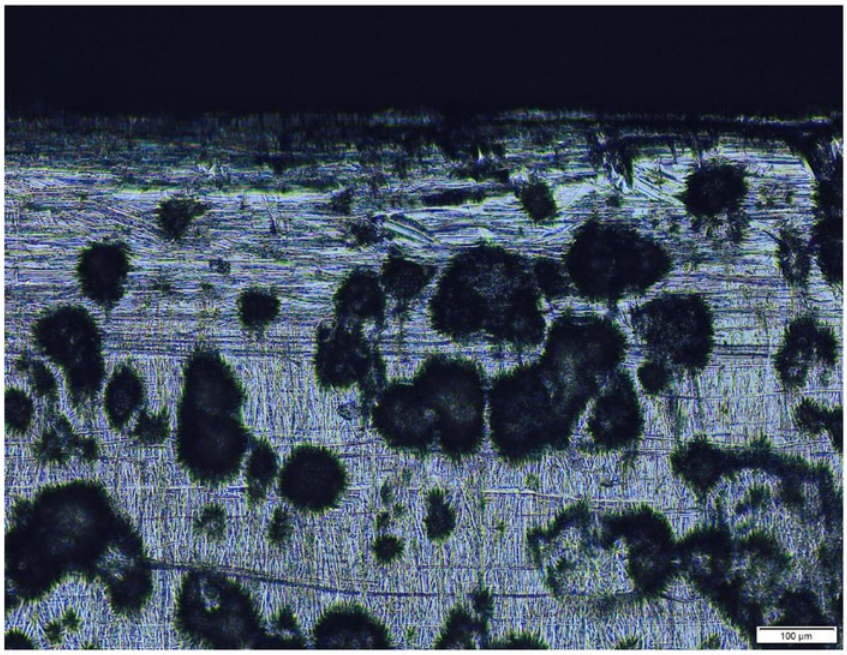

Figure 35 Corrosion and removal of material from surface of the die (100 µm Scale)

Here we can see areas of pitting on the die's surface These areas are similar to those shown in figures 19 and 80 in that they were taken from the die's surface. As shown in tables 8 and 9 these areas potentially contain molybdenum oxide, meaning the regions are harder and subsequently more brittle. During use they have the potential to break away causing degradation of the die and are likely responsible for the corrosion of the material shown above.

As highlighted above it is evident that monitoring the bearing surface of the die is critical. The main reason for its degradation is the failing of its bearing surface due to a lack of nitriding or other such surface treatment. In developing better wearing dies it is suggested that we look at ways to quickly ascertain the condition of the nitride coating that protects them. Whilst we already have the means to almost exactly determine the thickness and subsequent lifespan of such coatings through technologies such as powder x-ray diffraction and SEM analysis, both techniques possess limitations in terms of cost, time and practicality.

Moving forward in developing dies that are better wearing and longer lasting will require simplistic technologies that can be applied in the field to give a quick and accurate measurement of the depth of the nitride layer. From this we are able to gain an understanding of the condition of the nitride layer in terms of its thickness. This can then be directly related to its expected life, allowing us to determine when the re-application of a nitride treatment is needed to ensure the bearing surface is not degraded during extrusion.

One method I looked at to achieve this was through the use of hardness testing. As noted, a hardness test gives a reading based on the level of deformation at a specific test point. The rationale behind this method is that the surface of the die has been nitrided. This means it is significantly harder than the substrate material. Using the same test force, an indent made on the nitrided section of the die will be considerably smaller in size when compared to one made on a section of the die where there is either no nitride treatment or where it has begun to wear off.

A Vickers hardness test used for testing the dies allows for an optical measurement of this indent. Given the parameters for the diagonals and the overall hardness reading, we can accurately determine the depth of the indent. With the depth known we can easily ascertain the depth of this nitride layer, which is otherwise difficult to see.

Figure 36 below gives a visualisation as to how the process can be put into practice.

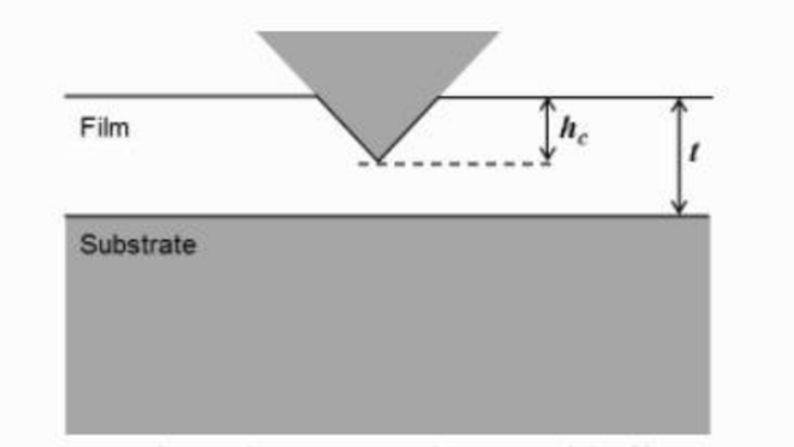

Figure 36 Measuring nitride layer depth through hardness test[2]

An initial hardness test should be made on a die to gauge its hardness. After heat treatment, the geometry of the indent and hardness reading should be recorded for reference. The die is then nitrided and the same hardness test should be performed again with the same parameters recorded. The data collected from these two tests are the base line measurements for the minimum thickness of the nitride layer as well as the maximum. For quick reference the depth of indentation from the hardness testing can be taken as $1/7^{th}$ of the mean of the diagonals, however for increased accuracy the following formula should be employed.

$$h = \frac{D}{(2\sqrt{2}\tan\left(\frac{\theta}{2}\right))}$$

Where:

D = Mean of the diagonals (μm)

h = Depth of the Indent (μm)

θ = Angle of Indenter (For Vickers $\theta = 136°$) (RAD)

There are some pitfalls to this method however. In general when talking about the thickness of a nitride layer on an extrusion die we are measuring in microns. When conducting the hardness test an appropriate amount of force must be selected for the test. In the event that a larger test force is used, we will see the indenter pass completely through the nitride layer and enter the substrate material. This will give a low hardness reading and an inaccurate result, hence a series of tests need to be conducted in order to first gauge the thickness of the nitride layer. The results of such as test can be seen in the tables below.

Table 13 Hardness indent depth calculations for surface of die for sample shown in figure 23

LOAD(Kgf)	D1(μm)	D2(μm)	HV	Mean Diagonal Length(μm)	Depth of Indent (μm)
0.5	35.5	34.5	757	35	4.9996
0.5	35.8	36.3	713	36.05	5.1495
0.5	37.4	35.8	693	36.6	5.2281
0.5	35.3	36.3	724	35.8	5.1138
0.5	35.3	34	774	34.65	4.9496
0.5	34.5	38.2	703	36.35	5.1924
1	51.8	53.7	666	52.75	7.5350
1	52.1	51.8	686	51.95	7.4208
1	52.6	51.3	686	51.95	7.4208
1	53.4	52.1	667	52.75	7.5350
1	52.4	50	708	51.2	7.3136
2	76.1	78	625	77.05	11.0062
2	76.6	74.7	648	75.65	10.8062
2	71.6	74.5	695	73.05	10.4348
2	79.5	81.4	573	80.45	11.4918
2.5	86.8	87.9	607	87.35	12.4775
2.5	85.3	88.5	614	86.9	12.4132
2.5	87.9	89.7	588	88.8	12.6846
2.5	91.1	89.7	567	90.4	12.9131
3	99.5	96.1	582	97.8	13.9702
3	96.1	97.4	595	96.75	13.8202
3	96.3	100.5	574	98.4	14.0559
3	93.4	95.8	622	94.6	13.5131

What we see from table 13 is exactly what was mentioned previously. This sample as we know is nitrided and was not subjected to any of the forces caused by extrusion, hence the nitride layer is still complete and intact. What the results show us is that when we applied the 0.5 kgf force we saw our greatest recorded hardness and average indent depth of 5.11μm. As the force of the indenter increased, the hardness decreased and subsequently the indent depth increased. This was due to the fact that the indenter was now passing through the nitride layer and beginning to enter the substrate material.

In order to show this trend is in fact an accurate way to measure the nitride depth on the die, I repeated the test. This time I tested it on a region of the die I had examined using SEM and had visually seen that the nitride layer had completely worn off.

Table 14 Hardness indent depth calculations for Sample 1 lot 1

LOAD(Kgf)	D1	D2	HV	Mean Diagonal Length (μm)	Depth of Indent (μm)
0.5	41.9	42.4	522	42.15	6.0209
0.5	42.9	41.8	517	42.35	6.0495
0.5	41.9	42.4	522	42.15	6.0209
0.5	44.3	44.8	468	44.55	6.3637
0.5	41.1	41.6	543	41.35	5.9066
0.5	40.3	41.8	550	41.05	5.8638
1	57.6	59	546	58.3	8.3278
1	59.5	60	520	59.75	8.5350
1	57.9	57.3	558	57.6	8.2278
1	58.7	60.8	520	59.75	8.5350
2	90.6	88.4	463	89.5	12.7846
2	84.2	84.5	521	84.35	12.0489
2	83.2	85.6	521	84.4	12.0561
2	84.2	86.3	510	85.25	12.1775
2.5	93.7	94.7	522	94.2	13.4559
2.5	97.1	97.9	488	97.5	13.9273
2.5	98.7	101.3	463	100	14.2844
2.5	93.9	92.9	531	93.4	13.3417
3	103.4	105.3	511	104.35	14.9058
3	95.4	92.7	629	94.05	13.4345
3	110	108.2	468	109.1	15.5843
3	106.1	103.4	507	104.75	14.9629

As can be seen from table 14, when we have a sample with no case-hardened layer, increasing the indenter force does nothing to affect the hardness reading as the material hardness is homogenous in nature from here on. Inferring from the data in table 14 it can be seen that as the indenter force is increased the depth of the indent increases respectively, however the hardness remains the same. To further clarify this point the data from tables 13 and 14 were graphed below enabling us to observe the reported trends.

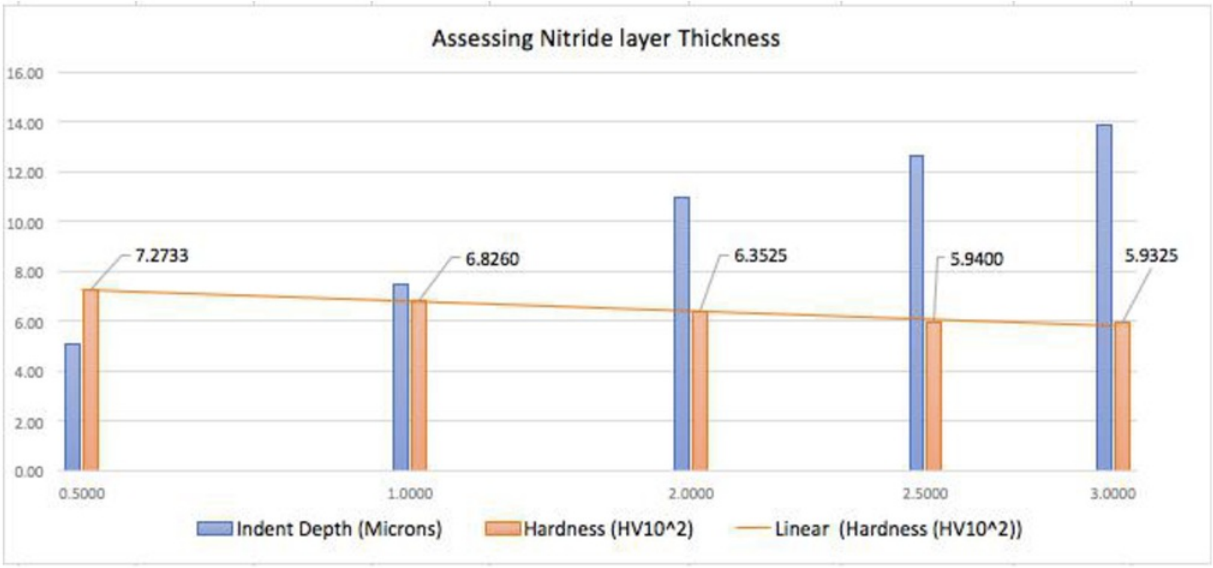

Figure 38 Graphical representation of data in table 13. Shows trend of increasing hardness indent depth with increasing test force, leading to a decreasing overall hardness for nitrided sample.

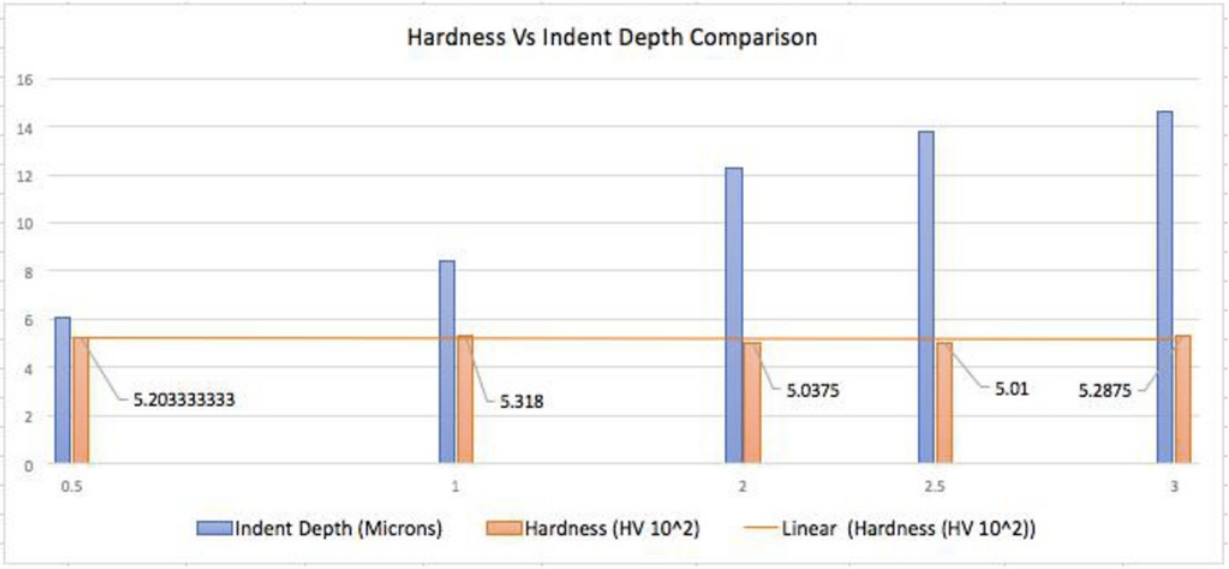

Figure 37 Graphical representation of data in table 14. Shows the trend of consistent hardness readings with increasing indenter force, for non nitride samples.

By comparing the trend lines of the two graphs the idea behind the method is evident. We must firstly establish a base hardness reading for a newly nitrided die. To do this we would test the sample with the smallest possible hardness indenter load that still allowed for an accurate hardness reading. In the case of this die it was 0.5Kgf. Smaller loads were tested, however the indenter failed to leave two clear diagonals and I was therefore unable to obtain an accurate hardness reading. Following on from this, the load on the indenter can be increased in predetermined increments. Based on the above results we would observe a decrease in hardness and an increase in the depth or indentation as the indenter begins to pass through the hardened layer and faces less resistance. Once the microhardness readings obtained from this method match that of the microhardness readings of the die obtained before the nitride layer, we know that the material will be homogeneous in nature from this point onwards. This means that we have successfully measured the total case depth and hence know the thickness of the coating.

As a way to check this method I took that same sample used in table 13 and examined it under the microscope hoping to observe the depth of the nitride layer.

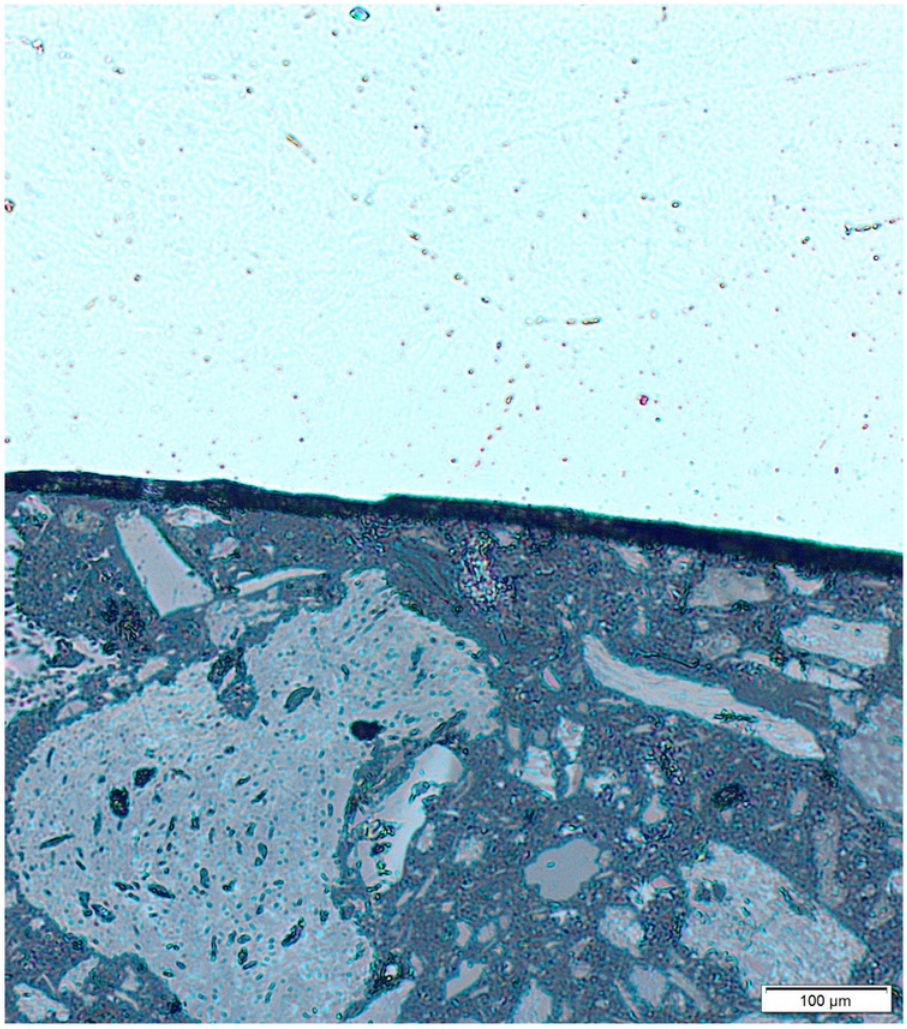

Figure 39 Visualisation and graphical measurement of nitride layer thickness

When looking at figure 39 what we are seeing is in fact the nitride layer and the substrate beneath it. The white region in the top half of the image is the underlying material beneath the bearing surface. Its white appearance is due to a lack in nitriding. The darker line that appears to separate the image is in fact the nitride layer. Its darker appearance is due to a difference in microstructure between it and the material beneath it. Looking at the scale on the image representing 100 microns, and comparing it to the results obtained in table 13, the table suggests the total case depth of the nitride layer to be 5-10 microns. Comparing this to figure … we 39 can see this does in fact seem to be the case. We see slight variances in the nitride layer thickness along the length of the bearing surface which again matches the data in table 13.

6. CONCLUSION

When assessing the wear resistance and degradation of extrusion dies there are several external factors that need to be given considerable thought. Though the idea is always to operate the die in such a manner as to preserve it and make it last as long as possible, it is ultimately a systems engineering problem. Variances between systems and different operating procedures make it difficult to devise a one fit all solution to maximising the life of a die, this is all before even considering factors such as varying geometries between the different dies or differences in the die material itself.

From the research presented above, it is suggested that the key to an extrusion dies longevity lies within its mechanical properties. A large portion of these characteristics are attributed to various heat treatment procedures and the addition of one or more surface hardening techniques that are re applied over the life of the die.

Prior to conducting any experimentation, the project was approached with the mentality that though an alteration to the described heat treatment procedure, we could subsequently alter the dies microstructure and consequently its mechanical properties. It was thought that this could lead to better performing and slower wearing dies. Upon analysis as shown above, it became clear quite quickly that this was not the case. Examination of the heat treatments as described in table 3 and comparing this to the images obtained through SEM and optical light microscopy, it was clear that the dies had a highly consistent microstructure throughout. All tested samples displayed a layered 2-phase ferrite and cementite microstructure known as perlite, the perlite microstructure is entirely expected in accordance with the described treatment. One of the major contributing factors in an extended life of an extrusion die is high levels of hardness, the layered nature of a pearlite microstructure provides exactly this.

Moving forward with the project, it was decided that our best possible chance of making a noticeable improvement would be through the examination of the die for failures. Discovery of such points would allow for further investigation as to their cause, from here we could suggest preventative measures that could be used to increase the life of the die.

As shown in the results above all demonstrated failures of the die came about due to excessive wear on the bearing surface of the die, this prompted further investigation into the nitriding process applied to the die aimed at reducing wear along the bearing surface.

Our investigation concluded that there were several main mechanisms of failure throughout the die. It was firstly noted, that on all surfaces exposed to the extrusion process almost all of the nitride coating had worn off, leaving the bearing surface exposed during extrusion. Alongside this we also saw due to the increased temperature of extrusion, caused by both the preheating of the aluminium billet and the friction during extrusion, the generation of molybdenum oxide. As noted molybdenum oxide only forms at elevated temperatures (above 300°C). The fact that it was found not only on the bearing surface of the die but also on the side of the die which has no contact with the aluminium during extrusion, rules out the possibility of a chemical interaction meaning that the oxidation is solely a result of the increase in temperature. This harder substance within the material was noted to be more brittle and consequently broke off during extrusion also altering the geometry of the die. The categorisation as molybdenum oxide is fairly conclusive as shown by the EDS results in tables 8, 9, and 11, as well as the fact that all recorded instances of it were on samples taken from the exposed surface of the die.

Based off these findings it was concluded that moving forward in generating better wearing dies a different approach was needed. Simply trying to apply a generic procedure that produces a die with greater lifespan was impractical given the time constrains, we observed far better results could be obtained if each die was treated individually.

Given that the nitriding process for each die was not performed by the manufacturer (Austex dies), making a recommendation when to re-apply such a treatment is difficult. This links back to the idea that this is a systems engineering problem mentioned earlier. Each user will operate the die in a different manner, hence in order to generate a longer lasting die that would overcome the failures found in this report, I suggested the establishment of a method that allowed me quickly and accurately ascertain the case depth of the protective hardened layer, over various regions of the die.

In doing this we would then have a far more accurate way in which to measure the duration of time between the application of new nitriding treatments. Additionally, this process could be applied to any die operating in any system. In order to meet these needs I proposed the use of hardness testing as a way in which to measure case depth.

The results above show we were able to successfully gauge the thickness of the nitriding layer on the surface of the die. A major part in testing the die is to ensure it is done in a non-destructive manner or in such a way as to not affect the finish of the final extrusion. Our results found that hardness testing of the die would not even need to be carried out on the bearing surface of the die, we found testing on the face of the die would be sufficient as it is exposed to similar temperatures and forces during extrusion, and was observed to wear at a similar rate. A hardness test in this region would allow the user to quickly gauge a reading for the remaining thickness of the nitride surface layer.

From here the user then has almost a visual representation as to the condition of the nitride layer thickness. This allows for better calculation of the time duration between surface treatments. It was noted however that wear over the die is not entirely consistent the majority of these inconsistencies are attributed to its varying geometry, for more accurate representation it is suggested that multiple readings are taken from various locations to give a better representation of the nitride layer thickness.

The suggested process has significant advantages over other such methods used to measure case depth such as XRD and SEM analysis. Firstly, it is considerably more cost effective, and with the generation of a library of reference data as suggested in future work, it is quick and can be carried out on site with minimal equipment.

To conclude the following recommendations were made based off analysis of the results from the dies provided.

There are many external factors responsible for altering the degradation of an extrusion die. Because of this it is recommended that each should be treated as individual component within a larger system, with each system operating differently. Stating this, measurements should be made periodically assessing the remaining thickness of the nitride surface layer. Evaluating these thickness measurements will allow the user to have an understanding as to the current condition of the die as well as indicate when the re application of a nitride treatment is necessary. This in turn will allow the user to gain the longest possible life out of the extrusion die.

7. FUTURE WORK

Carrying on from this project it is noted that the individual testing of every extrusion die is a tedious process. To speed up the process and ultimately make it better for the end user it is suggested that a library of references is generated for the various die materials and nitriding treatments.

Each time a die is made with a varying composition a baseline hardness reading should be taken and recorded. When the die is nitrided several more hardness readings should be performed. Each time we should note the hardness, depth of indent and indenter force used as shown in tables 13-14. The hardness tests should them be repeated until we no longer see a change in micro hardness. It is at this point we know the total case depth.

Once a library of data such as this exists, on site hardness tests can then quickly performed on the dies. Comparing the data taken for the onsite test to a similar material in the library the user will have an idea as to remaining coating thickness.

Alongside this it is noted that the addition of molybdenum to the alloy is for increased hardness, however its oxidation has also been seen as a large point of failure for the dies. Future work in developing better wearing dies should include the testing of other materials to replay molybdenum in the alloy, metals with higher oxidation temperatures should be explored and tested to see if it results in less degradation during the extrusion process.

8. REFERENCES

1. Calphad.com, *Iron Carbon Phase Diagram*. 2006.
2. toolbox, N., *Model for thin films*. 2014.
3. Czerwinski, F., *Thermochemical Treatment of Metals.* Materials Science 2012.
4. Struers, *Tool Steels, Others (DiaPro, Application Note)*, M.N. 1462, Editor., Struers: e-Metalog.
5. Aluminium, C. *Aluminium Production Process*. 2012 [cited 2017 17/8]; Available from: http://www.capral.com.au/Aluminium-Production-Process.
6. Council, A.A. *Properties & Sustainability*. 2013 [cited 2017 17/8/2017]; Available from: http://aluminium.org.au/properties_and_sustainability.
7. ThomasBjörka, *Weat of surface treaded dies for aluminium extrusion - a case study.* Enslevier, 2001. **249**(3-4): p. 316-323.
8. Stratton, P., *Reducing the surface degredation of Aluminium extrusion dies During Preheating.* Journal of Materials Engineering and Performance, 2009: p. 623-626.
9. Yang, H.W., Jing Ling; Li, Min; Cai, Lan Rong, *Study on Structure and Property of H13 Steel With Electro-Spark Plasma Surface Reinforced in the Sprayed Mist Medium.* Applied Mechanics and Materials, 2014. **543-547**: p. 3896-3899.
10. Arain, A. *Heat treatment and Toughness Behavior of Tool Steels (D2 and H13) for Cutting Blades*. 1999.
11. K.Saha, P., *Aluminium Extrusion Technology*, A. Innternational, Editor. 2000.
12. Manna, R. *Heat Treatment*. 2012. 1-38.
13. Di Rosa, G., *Fluidized bed furnace*. 1984, Google Patents.
14. Austex, P.C. 2017.
15. AB, O.S. *Handbook Of Stainless Steel*. 2013. 11-24.
16. Meka, S.R., et al., *Generating duplex microstructures by nitriding; nitriding of iron based Fe–Mn alloy.* Materials Science and Technology, 2016. **32**(9): p. 883-889.
17. NITRIDED, G.K.e.a.W.B.O., *WEAR BEAHAVIOUR OF NITRIDED MICROSTRUCTURES OF AISI H13 DIES FOR HOT EXTRUSION OF ALUMINIUM.* Metalurgija, 2005. **45**(1): p. 21-29.
18. M.Yang, R.S.J., *Alloying Effects on the Gas Nitriding Process.* Journal of Materials Engineering and Performance, 2014. **23**(12): p. 4181-4186.
19. Coating, N.E. *Plasma Nitriding History and Process*. 2017 29/8/2017]; Available from: http://www.northeastcoating.com/products/plasma-nitriding/process.

20. T.Liapina, A.L., E.J.Mittemeijer, *Nitrogen redistribution in ε/γ′-iron nitride compound layers upon annealing.* Elsevier, 2003. **48**(12): p. 1643-1648.
21. Mittemeijer, T.L.L.J., *Phase transformations in iron-nitride compound layers upon low-temperature annealing: Diffusion kinetics of nitrogen in e- and γ′-iron nitrides*
. Metallurgical and Materials Transactions, 2005. **37**(2): p. 319-330.
22. Jordan, D. *Controlling Compound (White) Layer Formation During Vacuum Gas Nitriding*. 2010. 1-20.
23. Thomas Björk, R.W., Sture Hogmark, *Wear of surface treated dies for aluminium extrusion — a case study.* Enslevier, 2001. **240**: p. 316-323.
24. Rockett, A., *The materials science of semiconductors*. 2008, Springer US.
25. Thomas Bjork, R.W., Sture Hogmark,Jens Bergstrom, Per Hedenqvist c ¨, *Physical Vapour deposition duplex coating for aluminium extrusion dies.* Elsevier, 1999: p. 225-229.
26. Thomas Bjork , M.B., Richard Westergard , Sture Hogmark , Jens Bergstrom a, , *New physical vapour deposition coatings applied to extrusion dies.* Surface Coatings and Technology, 2001(146-147): p. 33-41.
27. R.Rodríguez-Baracaldo, J.A.B., E.S.Puchi-Cabrera, M.H.Staia, *High Temperature wear resistance of (TiAl)N PVD coating on untreated and gas nitrided AISI H13 steel with different heat treatments.* Wear, 2007. **262**(3-4).
28. *Case Depth Hardness Testing*. 2017 7/10/17]; Available from: http://www.hardnesstesters.com/test-types/case-depth-hardness-testing.
29. test, e. *NHD-Nitride Hardness Depth*. 2017; Available from: https://www.emcotest.com/en/the-world-of-hardness-testing/hardness-know-how/applications-tips/curve-measurements/nhd-nitriding-hardness-depth/.
30. Voort, G.V. *Revealing the Microstructure of Tool Steels*. 2012.
31. Technology, M. *Molybdenum*. 2016; Available from: http://www.mtialbany.com/metals/molybdenum/.

9. APPENDIX

[1] H13 Tool Steel Datasheet (Provided by Austex Dies)

WERKSZEUGNIS
TEST REPORT
RELEVE DE CONTROLE
EN 10204-2.2

ISO 9001:2008 certification
EN ISO 14001:2004 certification

BÖHLER
EDELSTAHL

Cert. No.: 692135 / C2 / 2015.06.12
Blatt/Sheet/Page: 1 / 1

Besteller/Purchaser/Acheteur:
Company
Böhler Uddeholm (Australia) P/L
Suite 1, 25-27 Grose St
NORTH PARRAMATTA NSW 2151
AUSTRALIEN

Empfänger/Consignee/Destinaire:
Company
Böhler Uddeholm (Australia) P/L
Suite 1, 25-27 Grose St
NORTH PARRAMATTA NSW 2151
AUSTRALIEN

Bestell-Nr./Purchaser order No./No. de commande:
4800001462 / 2015.05.22

Empfängerref.-Nr./Receiver reference-No./Référence destinaire:
-

Werksauftrags-Nr./Works order-No./No. de la commande de l'usine:
0002011093 / 2015.05.22

Lieferschein-Nr./Delivery note-No./Avisd'expedition du client:
51231529 / 2015.07.27

Prüfgegenstand/Object of test/Object d'examen:
BÖHLER W302 ISODISC W-Nr. 1.2344
bar, forged, annealed max. 229 HB, IBO ECOMAX
ISO 286/2 ITk14
Endcondition: 1x cold cut/1x hot cut

Anforderungen/Requirements/Exigence:
BUAU WOL EST #
WH240

Umfang der Lieferung/Volume of delivery/liste descriptive

Pos./Los	Abmessung Dimensions Dimensions	Länge Length Longueur	Stückzahl No. of Pieces No. de Pieces	Gewicht kg Weight kgs Poids kg	Mat.-ID	Prüf-Nr. Test No. Eprouvette	Schmelze-Nr. Heat No. No. de coulee
70/1	RD 383 mm	random lengths 2000 - 5000 mm	1	2888,0	FYWN	1422084-1	A11634

Chemische Zusammensetzung/Chemical Composition/Composition chimique (%)

Schmelzanalyse/Chemical Composition Erschmelzungsart/Steelmaking Process: Airmelt								Schmelze-Nr. Heat No. No. de coulee
C	Si	Mn	P	S	Cr	Mo	V	
0,39	0,99	0,36	0,019	0,0004	5,06	1,23	0,95	A11634

Mechanische Eigenschaften/Mechanical Properties/Characteristiques mechaniques

Pos./Los	Härte / Zugfestigkeit Hardness / Tensile Strength Durete / Résistance à la traction		Prüf-Nr. Test No. Eprouvette
70/1	191	HBW	1422084-1

Radioaktivitätskontrolle/Radioactivity inspection: Co-60<0,1Bq/g;
hiermit kleiner als Grenzwert in der anzuwendenden Spezifikation IAEA RS-G-1.7 für unbedenkliche Stoffe.
therefore smaller than upper limit required according to specification IAEA RS-G-1.7 for inoffensive material.

Wir bestätigen hiermit, dass die obengenannten Erzeugnisse den Bestellvorschriften entsprechen.
We hereby certify that the above mentioned products are consistent with the order prescriptions.
Nous certifions que les produits enumeres ci-dessus sont conformes aux prescriptions de la commande.

BOHLER Edelstahl GmbH & Co KG
Mariazellerstrasse 25
8605 Kapfenberg, AUSTRIA
www.bohler-edelstahl.com
REGISTRIERGERICHT LANDESGERICHT

Abteilung / Department
VLO / Order Processing Center

AUSSTELLER /

GRAF

DER ABNAHMEBEAUFTRAGTE/

[2] Attendance Form

Consultation Meetings Attendance Form

Week	Date	Comments (if applicable)	Student's Signature	Supervisor's Signature
2	8/8/17.	CUTTING DIES / SOURCE POSSIBLE ETCHANT.		
3	15/8/17.	CONTACT AUSTEX GET HEAT TREAT METHOD.		
4	22/8/17	LOOK UP ETCHANT.		
5	30/8/17.	M-UNIT GET IMAGES OF MICROSTRUCTURE		
6	5/9/17	LOOK AT MOLYBENDUM CONCENTRATIONS.		
7.	13/9/17.	POSSIBLE CONTAMINATION OF POLISHING PAD. SEE IF WE HAVE ANOTHER.		
8	19/9/17	SEE IF WE CAN DO COMPOSITION MAPPING ON SAMPLE		
9	6/10/17	TALK TO AUSTEX ABOUT A NEW DIE FOR POSSIBLE COMPARISON.		
10	10/10/17	LOOK AT WAYS TO MEASURE THICKNESS OF THIN COATINGS.		
11	18/10/17.	GET EDS RESULTS LOOK FOR N ON DIE SURFACE.		
12.	24/10/17.	HAVE THESIS DONE READY TO BE CHECKED NEXT WEEK.		
13	31/10/17.	REMINDER → PRESENTATION NOTES!		